Lysosomal degradation of ACVR1-Activin complexes negatively regulates signaling of Activins and Bone Morphogenetic Proteins

Warren W. Hom, Senem Aykul, Lampros Panagis, Krunal Patel, Susannah Brydges, Erich J. Goebel, Kaitlin N. Hart, John B. Lees-Shepard, Sarah J. Hatsell, Vincent Idone, and Aris N. Economides

Regeneron Pharmaceuticals, 777 Old Saw Mill River Road, Tarrytown, NY 10591

Abstract
BMP/TGFß family ligands have mainly been studied as factors that initiate Smad signaling. Activin A stands out as it initiates Smad2/3 signaling through ACVR1B, whereas it generates non-signaling complexes (NSCs) with ACVR1 which can inhibit ACVR1-mediated BMP signaling. In the genetic disorder fibrodysplasia ossificans progressiva (FOP), which is caused by missense mutations in ACVR1 (ACVR1.FOP), Activin•ACVR1.FOP•type II receptor complexes activate Smad1/5 signaling, mimicking those formed with BMPs. As the NSCs that Activin A forms with ACVR1 are stoichiometrically identical with the signaling complexes formed with ACVR1.FOP, we explored how NSCs differ from their signaling counterparts. We demonstrate that NSCs rapidly traffic to the lysosome and are degraded, thereby reducing Activin A levels, in addition to removing ACVR1 and associated type II receptors. Hence, Activin-ACVR1 NSCs negatively regulate both the availability of Activin A and the level of BMP signaling mediated by ACVR1. Hence, lysosomal trafficking and degradation of NSC is a novel regulatory mechanism of BMP/TGFß signaling whose physiological roles remain largely unexplored.

Introduction

BMPs and TGFßs have primarily been studied as factors that initiate Smad signaling through heterotetrameric complexes of their corresponding type I and type II receptors [1-4]. BMP3, lefty1, lefty2, Inhibin A, and Inhibin B stand as exceptions as they function solely as antagonists. This is accomplished by forming non-productive complexes with type II receptors, either alone [5, 6] or in combination with non-signaling coreceptors [7, 8], thereby rendering type II receptors unavailable for signaling.

Recently, a more complex picture emerged with the Activin subfamily during exploration of the molecular mechanisms that drive the pathophysiology of fibrodysplasia ossificans progressiva (FOP). FOP is an autosomal-dominant genetic disorder characterized by progressive and cumulation heterotopic bone formation of connective tissues [9], arising from heterozygous missense mutations in the region encoding the cytoplasmic domain of the type I BMP receptor ACVR1. The great majority of patients carry a variant altering Arginine 206 to Histidine (*ACVR1*^{R206H}) [10]. This amino acid change renders ACVR1.R206H responsive to Activin A (as well as Activin B, AB, and AC) [11, 12], a property shared with all other FOP-causing variants of ACVR1 (ACVR1.FOP) tested to date [12]. Importantly, inhibition of Activin A with a monoclonal antibody ameliorated heterotopic bone formation in FOP mice (*Acvr1*$^{R206H/+}$), resulting in exploration of Activin A as a drug target for FOP [11, 13-16].

From a molecular mechanism standpoint, this finding indicated that Activin A must interact with ACVR1, as had been initially described [17-19]. We discovered that wild type ACVR1 forms non-signaling complexes (NSCs) with Activin A together with associated type II receptors. These NSCs inhibit ACVR1-mediated BMP signaling [11]. However, efficient inhibition is not driven solely by occupancy of type II receptors by Activin A as had been previously suggested [20, 21] – rather it requires interaction of Activin with ACVR1 [22]. In addition to interacting with ACVR1, Activin A associates with a different type I receptor, ACVR1B [23-25] and activates Smad2/3 signaling [26, 27]. Hence, in contrast to BMP3, lefty 1, lefty 2, Inhibin A, and Inhibin B, which act solely as inhibitors of signaling, Activin A has a dual role: it inhibits BMP-induced Smad1/5 signaling mediated by ACVR1, whereas it activates Smad2/3 signaling from ACVR1B.

In our initial attempts to explore the physiological role of **ACVR1•Activin A•type II receptor** NSCs, we engineered an Activin A mutein, Activin A.Nod.F2TL (F2TL), that retains the ability to activate ACVR1B but cannot form NSCs with ACVR1 [22]. Although F2TL does not form NSCs with ACVR1 (indicating lack of binding), it is nonetheless able to activate Smad1/5 signaling via ACVR1.R206H. The reason for this is that ACVR1 exists in ligand-independent heterodimeric complexes with partner type II receptors [4]. Therefore, F2TL can still dimerize **ACVR1.R206H•type II receptor** heterodimers by binding the type II receptors, thereby driving the formation of a heterotetramer comprised of two ACVR1.R206H•type II receptor dimers even in the absence of a direct interaction with ACVR1. We took advantage of this property to explore the role of NSCs in FOP, by comparing the amount of heterotopic bone that forms in response to equivalent amounts of Activin A versus F2TL in FOP mice. As FOP is a heterozygous condition, we hypothesized that F2TL by escaping engagement into NSCs (that would be formed with ACVR1 expressed from the remaining wild type copy of *Acvr1*), and generate more heterotopic bone in an implant assay. FOP mice with F2TL implants generated approximately 6 times more heterotopic bone at the implant site compared with FOP mice receiving identical implants containing an equivalent amount of Activin A [22]. These data demonstrated that in FOP **ACVR1•Activin A•type II receptor** NSCs have a physiologically important function of reducing the level of signaling by ACVR1^{R206H} in response to Activin A and tempering the amount of heterotopic bone formed [22, 28]. However, these findings did not address the molecular mechanism by which NSCs bring about their effects. To address this question, we explored the fate of **ACVR1•Activin A•type II receptor** NSCs at the cellular level as well as and how NSCs affect signaling.

Results

Activin A-ACVR1 NSCs are endocytosed and traffic to lysosomes

To assess the fate of **ACVR1•Activin A•type II receptor** NSCs we generated versions of ACVR1 and Activin A that can be tracked using fluorescence microscopy. For ACVR1, we engineered fusion proteins, Halo-ACVR1-HiBiT and Halo-ACVR1.R206H-HiBiT, which are N-terminally tagged with Halo tag and C-terminally tagged with HiBiT tag. This enables tracking of Halo-ACVR1-HiBiT and Halo-ACVR1.R206H-HiBiT using the fluorescent ligand (AF660) which emits in the red spectrum. To avoid artifacts associated with overexpression [4] and to reduce competition from untagged ACVR1, we introduced these ACVR1 fusion proteins into *Acvr1* homozygous-null (*Acvr1*$^{-/-}$) mouse embryonic stem cells (mESCs), using lentiviral delivery. The fusion proteins expressed in mESCs (**Extended Data Fig. 1a**), localized on the cell surface (**Extended Data Fig. 1b,c**), and displayed the expected neoresponsiveness to Activin A and hyperresponsiveness to BMP7 when Halo-ACVR1.R206H-HiBiT was utilized instead of Halo-ACVR1-HiBiT as the type I receptor (**Extended Data Fig. 2a,b**). The level of expression of endogenous type II receptors as well as other type I receptors were unaffected by the expression of Halo-ACVR1-HiBiT and Halo-ACVR1.R206H-HiBiT (**Extended Data Fig. 3a**). Activin A and F2TL were rendered fluorescent by crosslinking fluorophore AF555 that emits in the yellow spectrum. These fluorescently labeled ligands activated signaling at levels equivalent to their unmodified counterparts, indicating that the fluorophore had not significantly altered interactions with their receptors (**Extended Data Fig. 4**).

Having validated these cell lines and ligands, we used them to explore the fate of different complexes involving Activin A. When *Acvr1*$^{-/-}$*; Tg[Halo-ACVR1-HiBiT]* mESCs are treated with Activin A-AF555, Halo-ACVR1-HiBiT along with Activin A-AF555, localize in punctate structures within the cytosol (**Fig. 1a**). In contrast, when *Acvr1*$^{-/-}$*; Tg[Halo-ACVR1.R206H-HiBiT]* mESCs are treated with Activin A-AF555, neither Halo-ACVR1.R206H-HiBiT nor Activin A are found in the cytosol at appreciable levels (**Fig. 1b**). Endocytosis of NSCs that form between Halo-ACVR1-HiBiT and Activin A-AF555 proceeds rapidly, being complete approximately 15 minutes after addition of ligand (**Fig. 2a; Extended Data Fig. 5**). Endocytosed NSCs traffic to the lysosome as they colocalize with LAMP1, a lysosomal marker (**Fig. 2b**). These results provide the first evidence that **ACVR1•Activin A•type II receptor** NSCs undergo endocytosis and traffic to lysosomes whereas their ACVR1.R206H counterparts (which signal in response to Activin A) do not.

To make certain that endocytosis of **ACVR1•Activin A•type II receptor** NSCs is not a property restricted to mESCs, we also tested whether Activin A-AF555 also internalizes in the osteoblast-like cell line W20 [29] and compared it to F2TL-AF555. In W20 cells, Activin A-AF555 localizes in punctate structures within the cytosol whereas F2TL-AF555 remains on the surface (**Extended Data Fig. 6)**, mirroring the results obtained in mESCs. These results indicate that endocytosis of **ACVR1•Activin A•type II receptor** NSCs is not a property restricted to one type of cell.

Lysosomal degradation of NSCs reduces responsiveness to BMPs

Since **ACVR1•Activin A•type II receptor** NSCs traffic to the lysosome, we tested whether the components of the complex are degraded. In HEK293 cells coexpressing myc-tagged ACVR1 (myc-ACVR1) and HA-tagged ACVR2B (HA-ACVR2B), addition of Activin A results in reduction of the majority of both myc-ACVR1 and HA-ACVR2B (**Fig. 3a)**. In contrast, with myc-ACVR1.R206H as the type I receptor, the levels of myc-ACVR1.R206H and HA-ACVR2B are not reduced after exposure to Activin A. This data is consistent with differential trafficking of the corresponding complexes where complexes with wild type ACVR1 traffic to lysosomes whereas complexes with ACVR1.R206H remain on the surface and escape degradation.

One of the predictions of these results is that high levels of Activin A will render cells unresponsive to BMP signaling via ACVR1 even after Activin A has been removed. To explore this prediction, we tested the effect of Activin A pretreatment (followed by its removal) on BMP7-initiated signaling in HEK293 cells coexpressing myc-ACVR1 and HA-ACVR2B. We treated these cells for 60 minutes with 10nM Activin A, removed any excess by washing with PBS, then introduced BMP7 and measured Smad1/5 phosphorylation. Activin A pretreatment resulted in a severe reduction of Smad1/5 phosphorylation in response to BMP7, 30 minutes after its addition. The cells recovered their ability to respond by 2 hours after exposure to Activin A (**Extended Data Fig. 7a,b**), presumably via replenishment of the degraded receptors by newly synthesized ones.

To make certain that these results are not an artifact of overexpression, we repeated this experiment in mESCs. We utilized mESCs that are homozygous-null for both *Bmpr1a* and *Bmpr1b* (*Bmpr1a*$^{-/-}$; *Bmpr1b*$^{-/-}$) to avoid a competing Smad1/5 signal from activation of these type I receptors and followed the same treatment protocol as for HEK293 cells. Activin A pretreatment resulted in severe reduction of Smad1/5 phosphorylation in response to BMP7, mirroring the data obtained in HEK293 cells. In mESCs that had been exposed to Activin A, 100 nM BMP7 was needed to achieve the same level of signaling as 10 nM BMP7 (i.e., 10-fold less) in cells that had not been exposed to Activin A (**Fig. 3b,c)**. We extended these observations in W20 cells, which naturally express higher levels of ACVR1 than mESCs along with comparable levels of BMPR1A (**Extended Data Fig. 7c**) and again followed the same treatment protocol. Consistent with results thus far, pretreatment of W20 cells with 10nM Activin limited their responsiveness to 10 nM BMP7 (**Extended Data Fig. 7d, e**). This effect was less pronounced with 50 nM BMP7 presumably due to signaling via BMPR1A [30, 31]. These results verify our initial demonstration that Activin A acts as an inhibitor of BMP signaling mediated by ACVR1 [11], and provide a new mechanistic insight. Specifically, that it is not merely occupancy of ACVR1•type II receptor heterocomplexes by Activin A but rather their induced lysosomal degradation that underlies inhibition of BMP signaling. Furthermore, these results indicate that this inhibition can be temporally sustained until lysosomally degraded receptors have been replenished by newly expressed ones.

Inhibition of NSC formation enhances Activin A signaling via ACVR1B

Another predicted outcome of the lysosomal degradation of the components of **ACVR1•Activin A•type II receptor** NSCs is that Activin A availability will also be reduced. Hence, we hypothesized that inhibition of Activin's interaction with ACVR1 (and its incorporation into NSCs) would enhance Activin A signaling via ACVR1B. To test this hypothesis, we treated W20 cells, with an ACVR1 antibody (REGN5168) that blocks the interaction of ACVR1 with its ligands [4]. Treatment with REGN5168 enhanced Smad2/3 signaling by Activin A (**Fig. 4**), consistent with a mechanism where blocking Activin A's incorporation into NSCs with ACVR1 increases its availability to interact with other proteins, such as ACVR1B.

NSC endocytosis requires interaction between ACVR1 and Activin A

To understand the requirements for NSC endocytosis we first explored the role of ACVR1. We employed F2TL as it cannot engage ACVR1 directly, yet can drive dimerization of preformed (ligand-independent) heterodimers of ACVR1 with type II receptors [4, 22]. When F2TL-AF555 is utilized as the ligand, Halo-ACVR1-HiBiT and F2TL fail to internalize (**Fig. 1a, 2b**), indicating that direct association between Activin A and ACVR1 is required for endocytosis. Hence, in the absence of a direct interaction of Activin A with ACVR1 there is no endocytosis of the resulting complexes.

Additionally, we interrogated whether ACVR1B participates in the endocytosis of Activin A. We generated mESCs that either lack ACVR1 and retain ACVR1B (*Acvr1*$^{-/-}$*; Acvr1b*$^{+/+}$) or retain ACVR1 and lack ACVR1B (*Acvr1*$^{+/+}$*; Acvr1b*$^{-/-}$) and followed endocytosis of Activin A-AF555. Loss of ACVR1B does not impact endocytosis of Activin A-AF555, and may even increase it, whereas loss of ACVR1

greatly reduces it (**Extended Data Fig. 8)**. These results indicate that ACVR1B is not required for NSC endocytosis and does not appear to participate in this process.

NSC endocytosis requires type II receptors

To explore further the molecular mechanism by which NSCs form and carry out their function we asked whether type II receptors are required. Although ACVR1 is associated with type II receptors in non-covalent, ligand-independent heterodimeric complexes [4, 32], we asked whether the association of ACVR1 with Activin A alone might be adequate to cause trafficking of the resulting complex to lysosomes, even though that association would be very transient [22]. To determine this, we engineered mESCs that lack all three type II receptors that Activin A has been shown to associate with, namely ACVR2A, ACVR2B, and BMPR2 (*Acvr2a*$^{-/-}$*; Acvr2b*$^{-/-}$*; Bmpr2*$^{-/-}$), and tested internalization of Activin A-AF555. Absence of these receptors result in a complete loss of internalization of Activin A (**Extended Data Fig. 9**). When the expression of ACVR2B was restored via lentiviral transfer of Halo-ACVR2B-HiBiT to derive *Acvr2a*$^{-/-}$*; Acvr2b*$^{-/-}$*; Bmpr2*$^{-/-}$*; Tg[Halo-Acvr2b-HiBiT]* mESCs (**Extended Data Fig. 1a,c, 3b**), the response to Activin A was restored, with both Activin A and Halo-ACVR2B-HiBiT trafficking to the lysosome (**Fig. 5A, left panel**).

Signaling is not a determinant of NSC internalization

Given that stoichiometry of the **ACVR1•ligand•type II receptor** complexes is not a determinant of endocytosis, we explored whether signaling might be that determinant. To eliminate variables that could be introduced by varying the ligand, we engineered a mESC line wherein ACVR1.R206H was rendered kinase dead (ACVR1.R206H.K235R). We hypothesized that if signaling stops **ACVR1.R206H•Activin A•type II receptor** complexes from trafficking to the lysosome, then disabling that signaling by rendering ACVR1.R206H kinase dead the resulting **ACVR1.R206H.K245R•Activin A•type II receptor** complexes should mimic the NSCs formed with wild type ACVR1. Hence, we examined the trafficking of Activin A-AF555 and Halo-ACVR1.R206H.K235R-HiBiT in *Acvr1*$^{-/-}$*; Tg[Halo-Acvr1.R206H.K235R-HiBiT]* mESCs and compared it with its non-R206H kinase-dead counterpart, Halo-ACVR1.K235R-HiBiT in *Acvr1*$^{-/-}$*; Tg[Halo-Acvr1.K235R-HiBiT]* mESCs. In the presence of Activin A, Halo-ACVR1.K235R-HiBiT trafficked to lysosomes, whereas Halo-ACVR1.R206H.K235R-HiBiT remained on the surface (**Fig. 5b**). Hence, the complex of **ACVR1.R206H.K235R•Activin A•type II receptor,** which is unable to signal, retains the properties of its signaling counterpart – **ACVR1.R206H•Activin A•type II receptor** complex – rather than adopt the properties of **ACVR1•Activin A•type II receptor** NSCs.

Similar results were obtained via pharmacological inhibition of ACVR1 kinase activity using the small molecule LDN214117 [33], which very efficiently blocks Activin A-induced Samd1/5/8 signaling from ACVR1.R206H while leaving activation of Smad2/3 signaling via ACVR1B unaffected (**Fig. 6a)**. Inhibition of ACVR1 kinase in *Acvr1*$^{-/-}$ *; Tg[Halo-Acvr1.R206H-HiBiT]* mESCs does not result in endocytosis of **ACVR1.R206H•Activin A•type II receptor** complexes. Furthermore, inhibition of ACVR1 kinase in *Acvr1*$^{-/-}$ *; Tg[Halo-Acvr1-HiBiT]* mESCs, does not affect endocytosis and trafficking to the lysosome of **ACVR1•Activin A•type II receptor** complexes (**Fig. 6b**).

We also explored whether the kinase activity of type II receptors is required for endocytosis of NSCs. To this effect, we introduced Halo-ACVR2B-HiBiT or its kinase-dead counterpart, Halo-ACVR2B.K241R-HiBiT into *Acvr2a*$^{-/-}$*; Acvr2b*$^{-/-}$*; Bmpr2*$^{-/-}$ mESCs. The resulting lines were tested for responsiveness to BMP7. *Acvr2a*$^{-/-}$*; Acvr2b*$^{-/-}$*; Bmpr2*$^{-/-}$*; Tg[Halo-ACVR2B-HiBiT]* mESCs respond to BMP7 whereas *Acvr2a*$^{-/-}$*; Acvr2b*$^{-/-}$*; Bmpr2*$^{-/-}$*; Tg[Halo-ACVR2B.K241R-HiBiT]* mESCs do not **(Extended Data Fig. 10)**. We then tested their ability to internalize Activin A-AF555. Lack of ACVR2B kinase activity had no obvious effect on the internalization of Activin A-AF555 (**Fig. 5a, right panel**). This data indicates that signaling is not a determinant of trafficking of NSCs to the lysosome; rather a different mechanism must be involved.

Other Activins also form NSCs with ACVR1 and suppress BMP signaling
Since Activin AB, B, and AC can activate signaling of ACVR1.R206H, we surmised that those ligands must also form NSCs with wild type ACVR1. Hence, we tested whether Activin AB, B, AC, as well as Activin E can inhibit BMP7-induced signaling via ACVR1. First, we qualified that these ligands could activate ACVR1.R206H. Whereas Activin AB, B, and AC activate signaling via ACVR1.206H, Activin E does not (**Fig. 7a)**. None of these ligands activate signaling in HEK293 cells overexpressing wild type ACVR1 (**Fig. 7b**). Activin AB and B repress BMP7-induced signaling similarly to Activin A, whereas Activin AC is less efficient (**Fig. 7c**). Activin E cannot inhibit signaling at appreciable levels, presumably because it does not interact with ACVR1. We attribute the mild inhibition achieved at high levels of Activin E to occupancy of type II receptors. Similar results were obtained in *Bmpr1a*$^{-/-}$; *Bmpr1b*$^{-/-}$ mESCs, where ACVR1 is not overexpressed. mESCs were treated with the different Activins for 60 minutes, then excess ligands were removed with washing, and subsequently the cells were exposed to BMP7 for 30 minutes. All the Activins except Activin E suppressed BMP7-induced signaling (**Fig. 7d**). These results indicate that ACVR1 can form NSCs with several other Activins, and these NSCs appear to behave similarly to those formed in the presence of Activin A.

Discussion

We have reported here a novel regulatory mechanism in the BMP/TGFß pathway. Activin A and ACVR1 coordinately regulate their own signaling by forming **ACVR1•Activin A•type II receptor** NSCs that are rapidly endocytosed and traffic to the lysosome (**Fig. 8**). Conversely, identical complexes utilizing FOP-causing variant ACVR1.R206H remain on the membrane and signal. This stands in contrast to another Activin receptor, ACVR1B, which appears to cycle between the membrane and early endosomes irrespective of engagement by ligand [34].

In the lysosome, the NSC's components are degraded, resulting in a reduction in ACVR1 and associated type II receptors [4] on the cell surface. Consequently, in the presence of Activin A, BMP signaling through ACVR1 is reduced. This effect can be sustained, with cells treated with Activin A remaining unresponsive to subsequent stimulation by BMPs until ACVR1 and type II receptors have been replenished. The degree to which BMP signaling is suppressed depends on the expression level of ACVR1 relative to other type I BMP receptors: in cells where the main type I BMP receptor is ACVR1, signaling by BMPs is greatly inhibited, whereas in cells where other type I BMP receptors are expressed BMP signaling is less subject to the effects of NSCs.

Furthermore, NSCs appear to be a mechanism that limits the amount of bioavailable Activin A. In cells where ACVR1 is highly expressed in comparison to ACVR1B, the responsiveness of the latter to Activin A is reduced. Conversely, inhibition of binding of Activin A to ACVR1 results in higher levels of signaling via ACVR1B. As antagonism is reciprocal, NSCs have the capacity to most potently regulate the more limiting component (ACVR1•type II receptor heterodimers versus Activin A). Our observations agree with a mathematical model showing that the outcome of signaling by any given set of ligands depends on the specific repertoire of receptors (both with respect to their identity and their relative abundance) in the responding cell [35]. These observations also pertain to Activin AB, B, and AC, as they also form NSCs with ACVR1, and they demonstrate that unlike most other BMP/TGFß family members which act solely as agonists or antagonists of signaling, these Activins have a dual role in that they can act as both agonists of Smad2/3 signaling and antagonists of Smad1/5 signaling through ACVR1.

Our findings have implications for therapeutic approaches targeting ACVR1 signaling in FOP and other indications. Various approaches are under investigation [36], including inhibition of Activin A [15], inhibition

of ACVR1 kinase [37-39], inhibition of ACVR1 using blocking antibodies [4, 16, 40-42], and siRNA-mediated reduction of ACVR1 expression [43]. Our findings predict that at the molecular level these approaches will have different outcomes. For example, inhibition of Activin A will not only abrogate activation of ACVR1.FOP, but also block the formation of Activin A-ACVR1 NSCs, whereas it will leave signaling by BMPs via ACVR1 unperturbed, and with the potential to be elevated. Inhibition of ACVR1's kinase activity will block signaling by both Activin A and BMPs via ACVR1 (whether FOP-variant or wild type) but will leave the formation of NSCs unperturbed. Inhibition of ACVR1 using antibodies will impact signaling and non-signaling complexes alike. Likewise, methods that decrease the expression of ACVR1, whether it is via siRNA, ASO, or gene editing will impact all ACVR1's functions equally unless they are allele specific.

Lastly, our findings have broader implications for BMP and Activin signaling as they indicate that the formation of heterotetrameric complexes of type I and type II receptors with ligand cannot be the sole determinant of signaling. The complexes that ACVR1 forms with BMPs or Activin A are stoichiometrically identical yet bring about very different outcomes, signaling versus trafficking to the lysosome, respectively. The same applies to complexes involving Activin A with ACVR1.FOP versus ACVR1. The molecular mechanism underlying this property is currently unknown, but it is likely to involve ligand-induced conformational changes. In addition to these molecular mechanism related questions, the physiological roles of NSCs outside of FOP remain to be elucidated. Given that loss of *Acvr1* [44-49] or *Inhba* [50] result in multiple phenotypes, it is possible that a subset may result from loss of NSC function rather than loss of signaling. We propose that elucidation of the molecular mechanisms driving phenotypes resulting from genetic alterations in either ACVR1 or any of the NSC-forming Activins should take into consideration both the ability of these proteins to acts as signaling molecules as well as their ability to suppress BMP signaling and/or regulate their own availability.

Figures

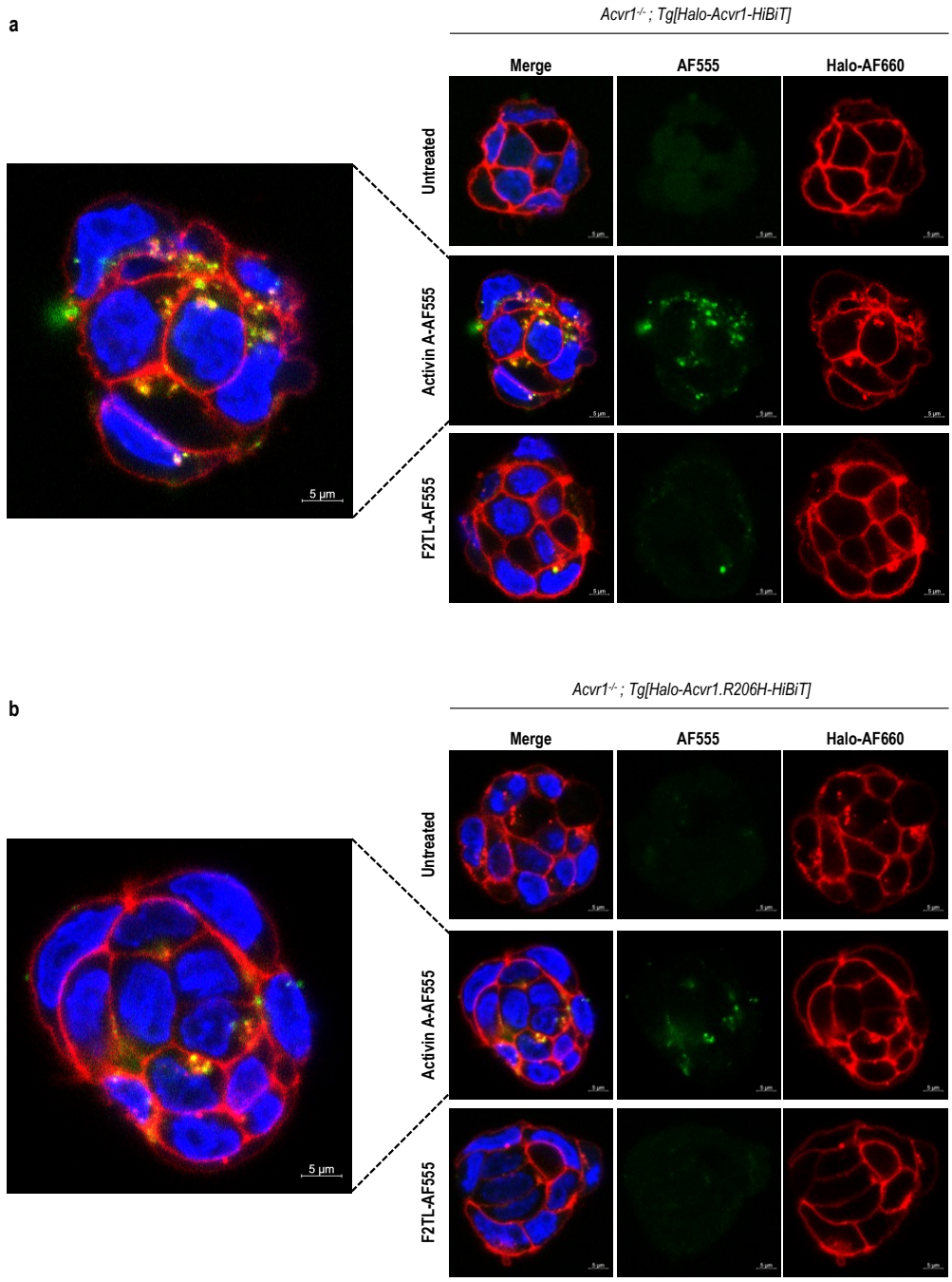

Figure 1. ACVR1•Activin A•type II receptor NSCs undergo endocytosis. a,**b**, *Acvr1*$^{-/-}$ mESCs expressing either Halo-ACVR1-HiBiT (**a**) or Halo-ACVR1.R206H-HiBiT (**b**) were treated with 30nM Activin A-AF555 or F2TL-AF555 or left untreated. ACVR1 proteins were visualized using AF660 Halo ligand (red). Nuclei were visualized using DAPI (blue). Activin A or F2TL were detected via the AF555 fluorophore (green). Confocal microscopy was used for imaging. Activin A-AF555 co-internalized with Halo-ACVR1-HiBiT but did not internalize with Halo-ACVR1.R206H-HiBiT. F2TL-AF555 did not drive endocytosis of either ACVR1 or ACVR1.R206H.

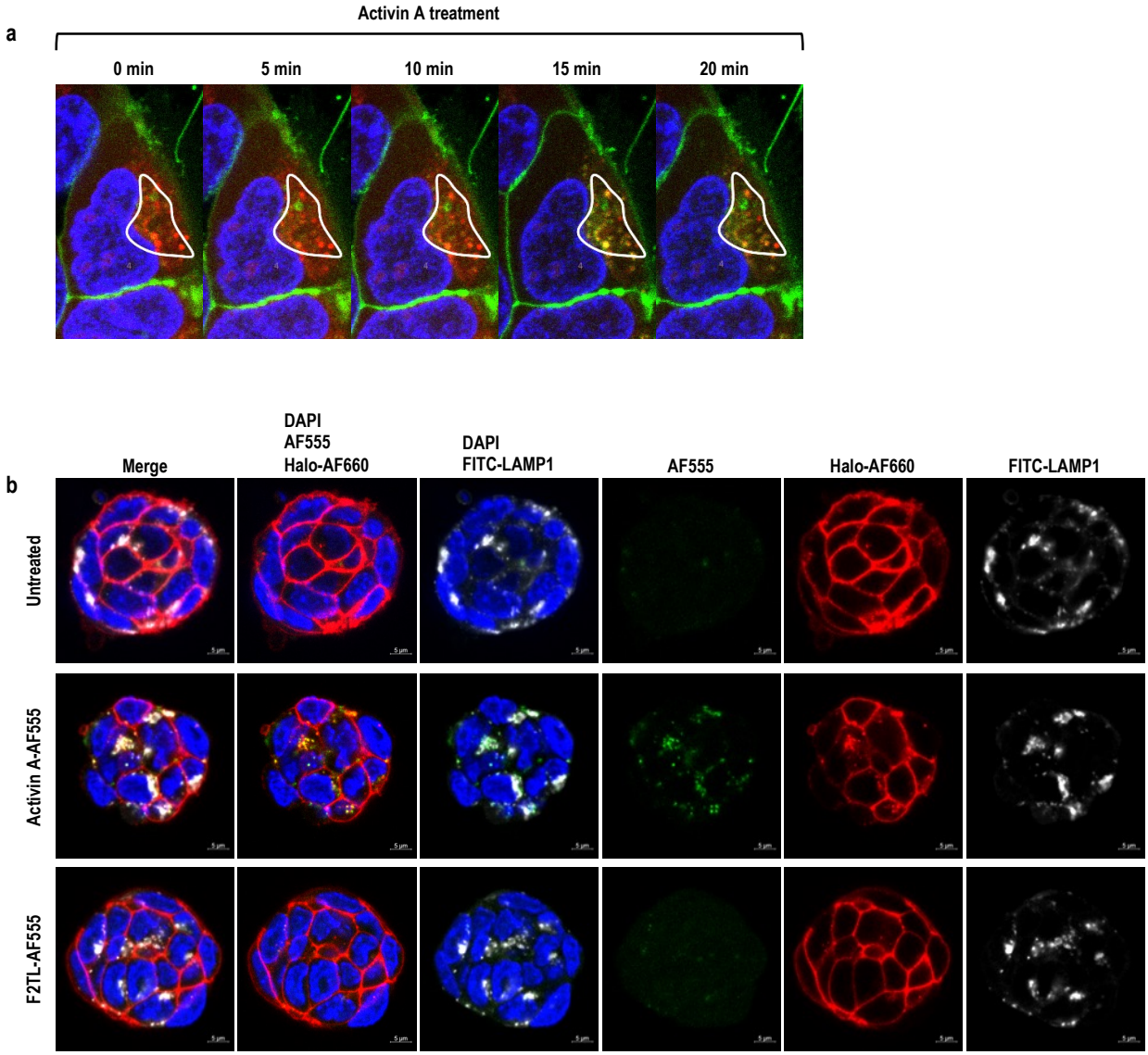

Figure 2. ACVR1•Activin A•type II receptor NSCs traffic to the lysosome. a, Live cell imaging of HEK293 cells overexpressing ACVR1-GFP (green) was performed post-lysosome staining with lysopainter (red). The GFP signal was bleached in the outlined area (white), followed by the addition of 30nM Activin A. Trafficking of ACVR1-GFP into lysosomes was monitored over a 30-minute period. Images from selected time points are displayed. ACVR1-GFP trafficked to the lysosome within 15 minutes after Activin A treatment. **b**, *Acvr1*$^{-/-}$ mESCs expressing Halo-ACVR1-HiBiT were treated with 30nM Activin A-AF555 (green) or left untreated. ACVR1 proteins were visualized using AF660 Halo ligand (red). Lysosomes and nuclei were visualized with FITC-LAMP1 (white) and DAPI (blue), respectively. Confocal microscopy was used for imaging. Activin A-AF555 co-internalized with Halo-ACVR1-HiBiT and localized in LAMP1-positive lysosomes. In contrast, F2TL-AF555 did not internalize in mESCs expressing Halo-ACVR1-HiBiT.

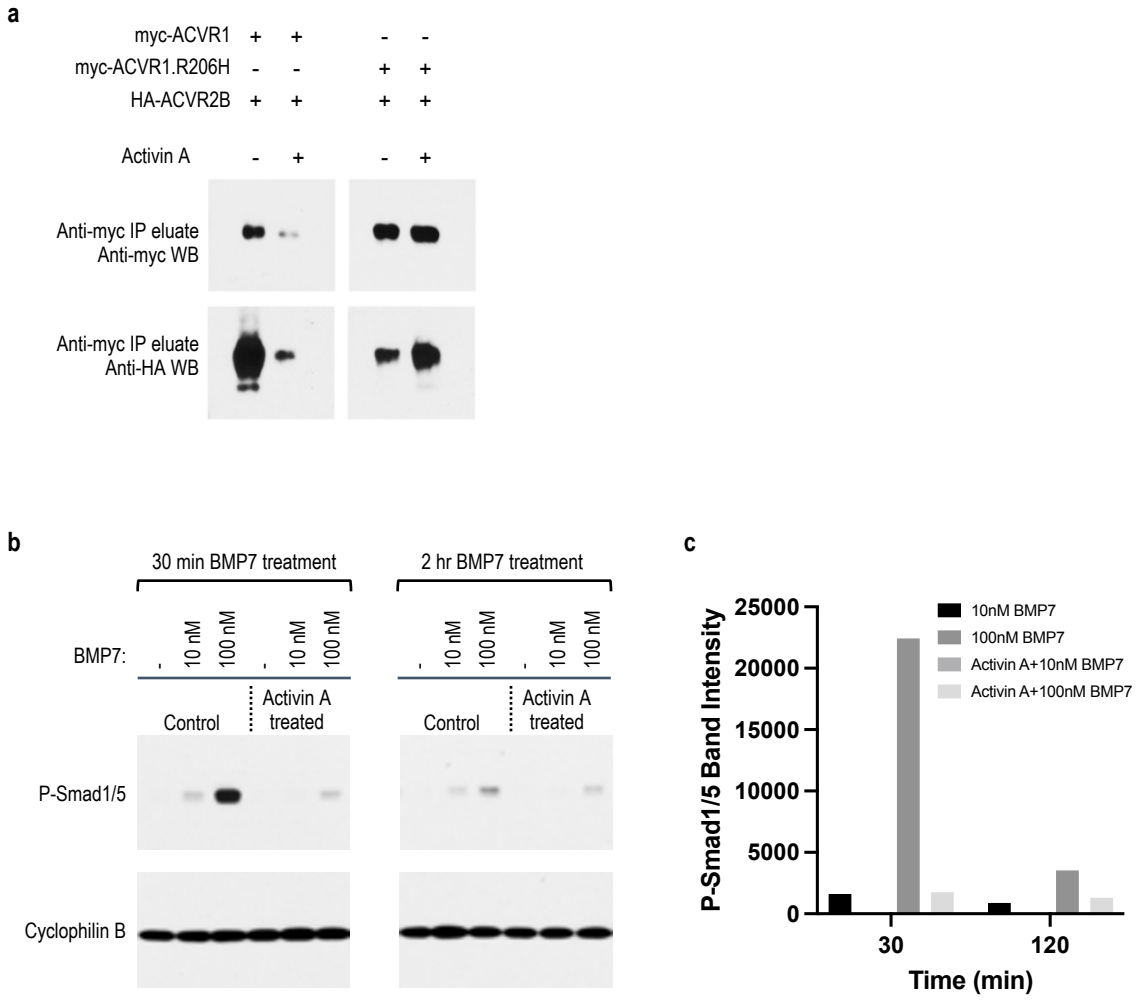

Figure 3. ACVR1•Activin A•type II receptor NSCs decrease BMP signaling by removing receptors from the cell surface. a, HEK293 cells were transiently transfected with either myc-ACVR1 or myc-ACVR1.R206H, in combination with HA-ACVR2B, and treated with Activin A, or left untreated. Membranes were isolated, normalized for protein concentration, and proteins were immunoprecipitated using anti-myc magnetic beads. HA-ACVR2B co-immunoprecipitated with myc-ACVR1 or myc-ACVR1.R206H. ACVR1 and ACVR2B were detected using Myc and HA antibodies, respectively. Exposure to Activin A resulted in a reduction of myc-ACVR1 and HA-ACVR2B in the membrane of cells expressing myc-ACVR1. Conversely, in cells expressing myc-ACVR1.R206H, both myc-ACVR1.R206H and ACVR2B levels do not change appreciably during exposure to Activin A. **b**,**c**, *Bmpr1a*$^{-/-}$; *Bmpr1b*$^{-/-}$ mESCs were either left untreated or treated with 10nM Activin A for 1 hour. After washing off unbound Activin A, cells were exposed to varying concentrations of BMP7 for either 30 minutes or 2 hours. Immunoblot analysis (**b**) and quantification (**c**) demonstrate that Activin A significantly decreases BMP7-induced Smad1/5 phosphorylation.

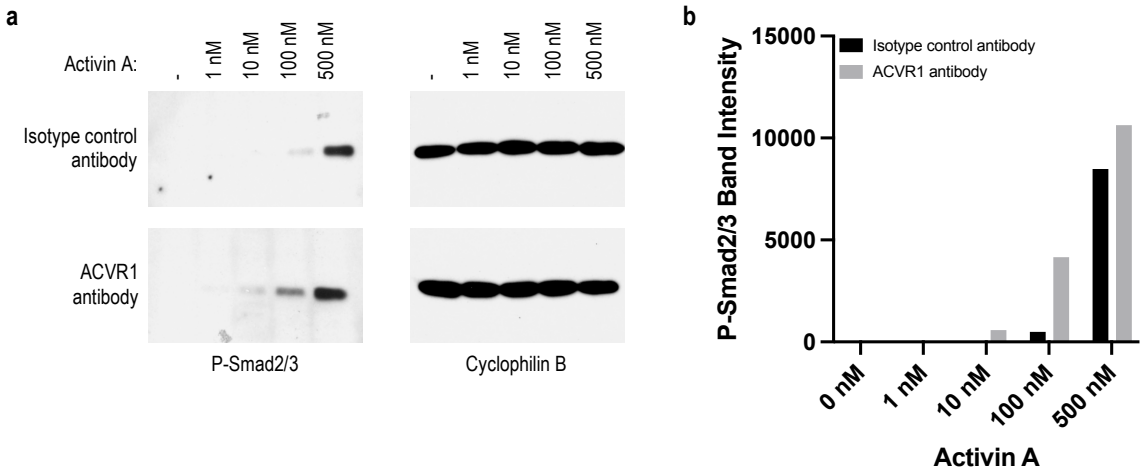

Figure 4. Blocking the binding of Activin A to ACVR1 increases Activin A availability and Smad2/3 signaling. a,**b**, W20 cells were treated with either 300nM isotype control antibody or ACVR1 blocking antibody for 1 hour, followed by the addition of varying concentrations of Activin A for another hour. Immunoblot analysis (**a**) and quantification (**b**) demonstrate that Activin A-induced Smad2/3 phosphorylation is increased in the cells treated with the ACVR1 antibody.

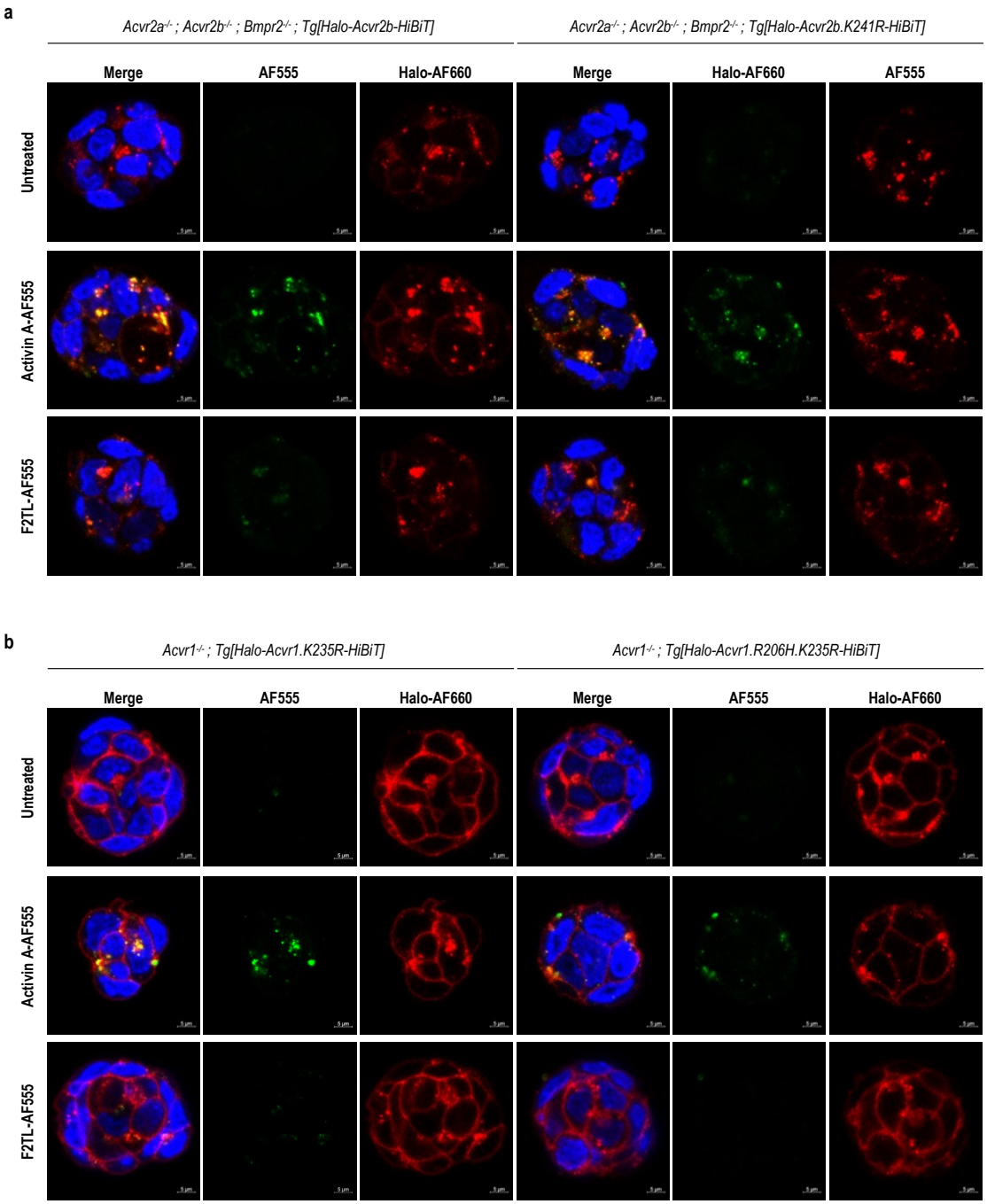

Figure 5. Signaling is not a determinant of NSC endocytosis. a,**b**, *Acvr2a*$^{-/-}$*; Acvr2b*$^{-/-}$*; Bmpr2*$^{-/-}$ mESCs expressing Halo-ACVR2B-HiBiT and Halo-ACVR2B.K241R-HiBiT (**a**), as well as *Acvr1*$^{-/-}$ mESCs expressing Halo-ACVR1.K235R-HiBiT and Halo-ACVR1.R206H.K235R-HiBiT (**b**) were either treated with 30nM Activin A-AF555 or F2TL-AF555 (green) or left untreated. ACVR1 and ACVR2B proteins were visualized with AF660 Halo ligand (red) and DAPI (blue). Confocal microscopy was used for imaging. Activin A-AF555 internalized in kinase-dead Halo-ACVR1.K235R-HiBiT, Halo-ACVR2B-HiBiT, and kinase-dead Halo-ACVR2B.K241R-HiBiT expressing mESCs, but not in kinase dead Halo-ACVR1.R206H.K235R-HiBiT expressing mESCs. F2TL-AF555 did not internalize in any of the tested mESC lines.

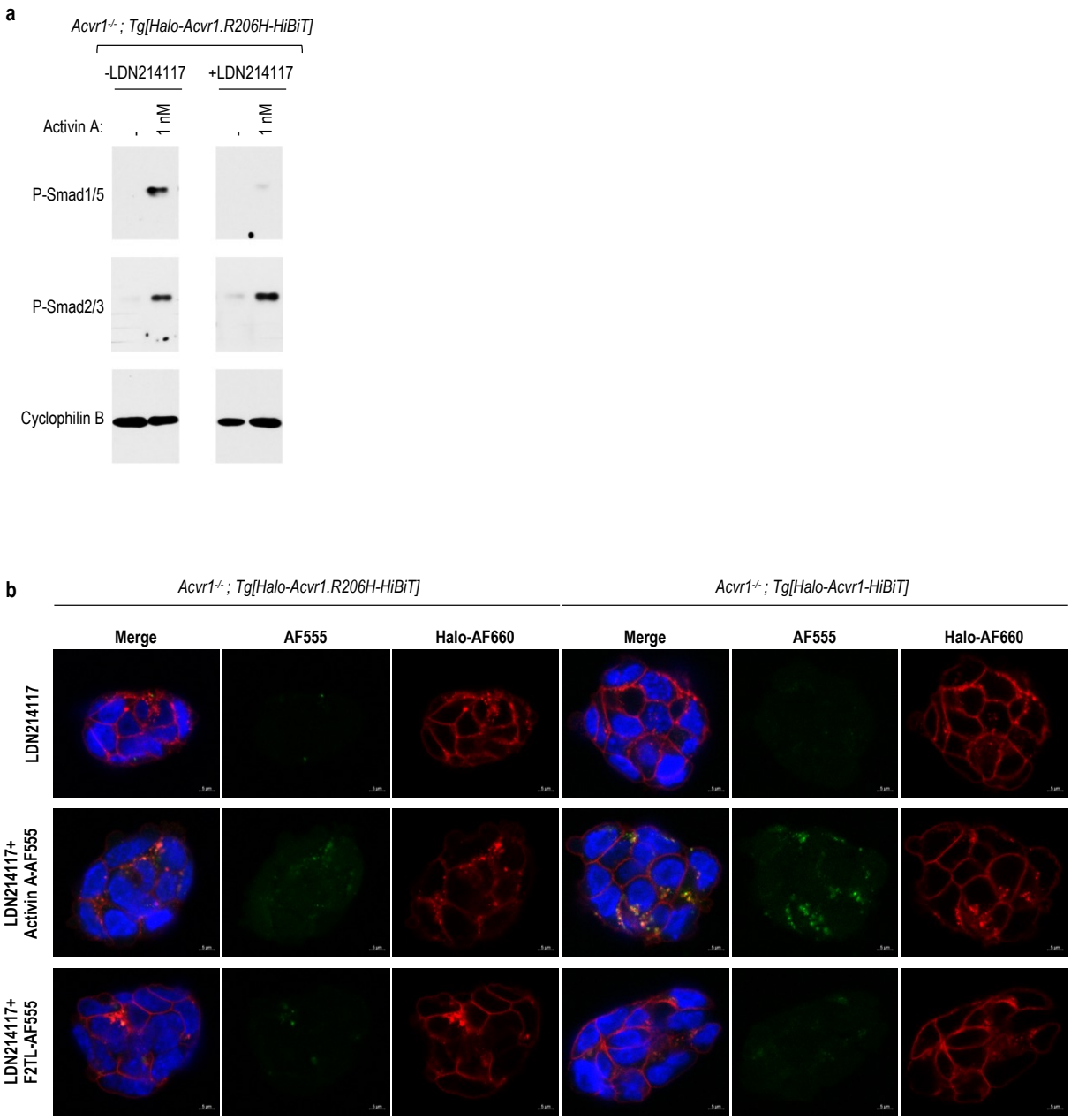

Figure 6. Inhibition of ACVR1.R206H kinase activity does not result in lysosomal trafficking of ACVR1.R206H•Activin A•type II receptor complexes. a, *Acvr1*$^{-/-}$ mESCs expressing Halo-ACVR1.R206H-HiBiT were treated with 10nM LDN214117 for 1 hour followed by the addition of 1nM Activin A for another hour. LDN214117 inhibited Activin A-induced Smad1/5 phosphorylation, but not Smad2/3 phosphorylation. **b**, *Acvr1*$^{-/-}$ mESCs expressing Halo-ACVR1-HiBiT and Halo-ACVR1.R206H-HiBiT were either treated with 10nM LDN214117 for 1 hour, followed by the addition of 30nM Activin A-AF555 or F2TL-AF555 (green). ACVR1 and ACVR2B proteins were visualized with AF660 Halo ligand (red) and DAPI (blue). Confocal microscopy was used for imaging. Activin A-AF555 did not internalize in the LDN214117 treated Halo-ACVR1.R206H-HiBiT expressing mESCs but did internalize in the LDN214117 treated Halo-ACVR1-HiBiT mESCs. F2TL-AF555 did not internalize under either condition.

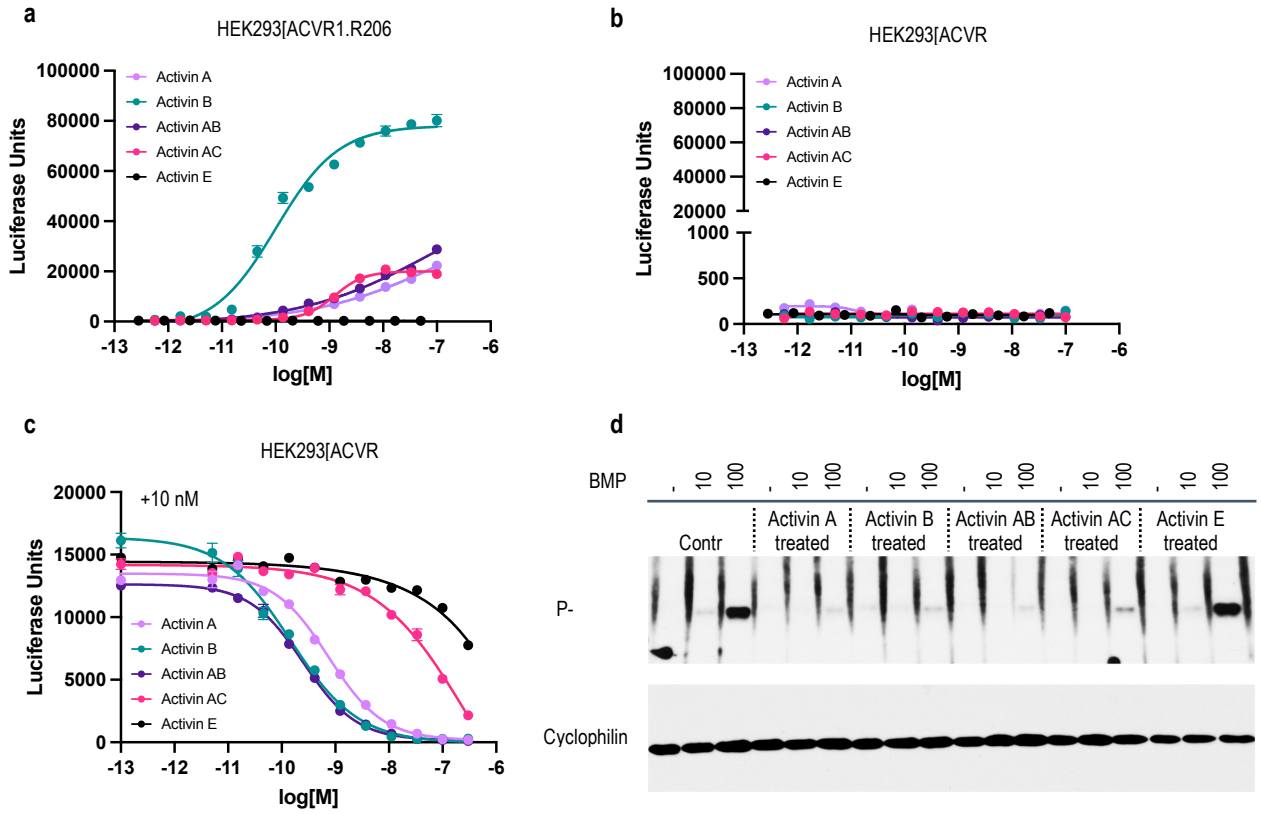

Figure 7. Other Activins also form NSCs with ACVR1 and suppress BMP signaling. a,**b**, Activin A, Activin B, Activin AB, Activin AC, and Activin E were titrated in the HEK293-BRE luciferase reporter cells (Smad1/5 responsive) overexpressing ACVR1.R206H (**a**) or wild type ACVR1 (**b**). None of the Activins induced Smad1/5 signaling in cells expressing the wild-type ACVR1. However, with the exception of Activin E, all other Activins induced Smad1/5 signaling in cells expressing the FOP mutant receptor ACVR1.R206H. **c**, HEK293-BRE luciferase reporter cells overexpressing wild type ACVR1 were treated with a fixed (10nM) concentration of BMP7, and different concentrations of Activin A, Activin B, Activin AB, Activin AC, or Activin E. Activins A, B, AB, and AC inhibited BMP7-induced Smad1/5 signaling, whereas Activin E did not. **d**, *Bmpr1a*$^{-/-}$; *Bmpr1b*$^{-/-}$ mESCs were either left untreated or treated with 10nM of Activins (Activin A, Activin B, Activin AB, Activin AC, and Activin E) for 1 hour. After washing off the unbound Activins, these cells were exposed to varying concentrations of BMP7 for 30 minutes. All Activins, except for Activin E, blocked BMP7-induced Smad1/5 phosphorylation.

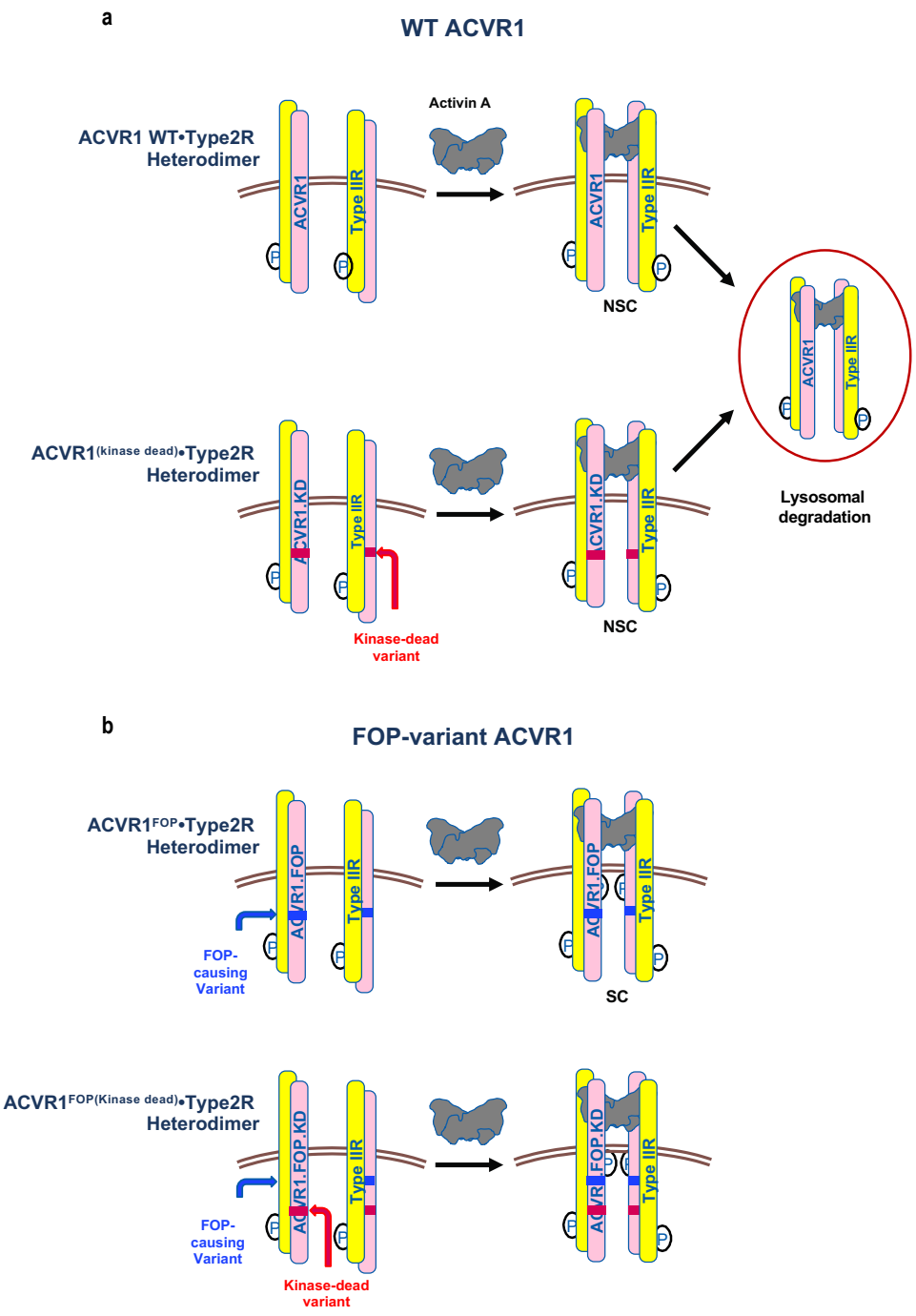

Figure 8. Activin and ACVR1 coordinately regulate their own availability. a, When Activin A binds wild type ACVR1 it drives the formation of NSCs that traffic to the lysosome wherein the components of the NSC are degraded. This results in a reduction of the NSC's constituent components and hence their availability for signaling. Trafficking of NSCs to the lysosome does not require kinase activity of either ACVR1 or type II receptor (not depicted). **b**, When Activin A engages FOP-variant ACVR1 such as ACVR1.R206H, the resulting complexes remain on the membrane and signal (SC). Conversion of these complexes into NSCs by rendering ACVR1.R206H kinase dead does not enable trafficking of ACVR1.R206H•Activin A•type II receptor complexes to the lysosome, indicating that signaling is not a determinant of this process.

Materials and Methods

Reagents

Activin A (338-AC-500/CF), Activin B (659-AB/CF), Activin AB (1066-AB-005/CF), Activin AC (4879-AC-010/CF), BMP7 (354-BP-010/CF), and anti-ALK4 antibody (MAB222) were purchased from R&D Systems. Activin E was custom produced. Activin A.Nod.F2TL (F2TL), anti–Activin A antibody (REGN2477), anti-ACVR1 antibody (REGN5168), and hIgG4 isotype control antibody were expressed and purified in-house. The Activin A-AF555 and F2TL-AF555 were generated in-house.

Generation and culturing of genetically modified mESCs

Acvr1$^{-/-}$, *Acvr1b*$^{-/-}$, *Bmpr1a*$^{-/-}$; *Bmpr1b*$^{-/-}$, and *Acvr2a*$^{-/-}$; *Acvr2b*$^{-/-}$; *Bmpr2*$^{-/-}$ mES cell lines were generated as previously described using CRISPR guides to biallelically ablate the target gene [4]. mESC lines were expanded on gelatin-coated flasks, layered with irradiated primary mouse embryonic fibroblast (MEF) feeder cells from the DR4 mouse strain, which is resistant to neomycin, hygromycin, puromycin, and 6-thioguanine (MilliporeSigma, PMEF-DR4X). mESCs were cultured in VG-DMEM media containing 15% (v/v) FBS, 50 U/mL penicillin/streptomycin, 0.2% (v/v) b-mercaptoethanol, and 2U/mL leukemia inhibitory factor (MilliporeSigma, ESG1107) in a 37°C humidified incubator with 5% CO_2. MEF feeder cells were removed using magnetic feeder removal microbeads (Miltenyi Biotec, 130-095-531) according to the manufacturer's protocol. After the removal of feeder cells, the mESCs were cultured in 2i media [51] on gelatin-coated plates.

Lentivirus and transduction of mESCs

Wild-type, mutant versions of HaloTag-mouse ACVR1-HiBiT, HaloTag-mouse ACVR1B-HiBiT and HaloTag-mouse ACVR2B-HiBiT lentiviruses were generated in HEK293T cells using Lenti-X Packaging Single Shots (Takara Bio, 631276) and concentrated 20-fold with Lenti Concentrator (OriGene, TR30025), in accordance with the manufacturers' instructions. A mixture of 50µL of concentrated lentivirus and 20µL LentiBlast Premium transduction enhancer (Oz Biosciences, LBPX500) was combined with 1 x 10^6 mESCs immediately after MEF feeder cell removal and then plated in gelatin-coated 6-well plates. After 48 hours, mESCs were transferred to gelatin coated T75 flasks containing MEF feeder cells to undergo antibiotic selection until stable cell lines were generated.

Flow cytometry

mESCs were non-enzymatically dissociated using Accutase solution (MilliporeSigma, A6964) and resuspended in flow cytometry staining buffer (Thermo Fisher Scientific, 50-112-9748) after the removal of feeder cells. Following a 15-minute blocking period (Thermo Fisher Scientific, 14-9161-73), cells were stained for one hour with 3.5µM HaloTag Alexa Fluor 660 ligand. This was followed by a viability staining (Thermo Fisher Scientific, L34955) for 30 minutes at a 1:1000 dilution. The stained cells were then fixed with CytoFix (BD Biosciences, 554655), passed through a filter block (Pall, PN 8027), and analyzed using a CytoFLEX LX flow cytometer (Beckman Coulter).

Confocal Microscopy

mESCs were plated in gelatin-coated 8-well chamber slides (Ibidi, 80826) in 2i media following the removal of feeder cells. After 48 hours, the 2i media was replaced with serum-free KnockOut DMEM (Thermo Fisher Scientific, 10829018) supplemented with 2mM L-glutamine, 50U/mL penicillin/streptomycin, 2 U/mL Leukemia Inhibitory Factor, and 0.1% bovine serum albumin (BSA) for 1 hour. During this incubation period, HaloTag-receptor expressing mESCs were fluorescently labeled with either 1 µM of HaloTag AlexaFluor 488 ligand (Promega, G1001) or 3.5µM of HaloTag AlexaFluor 660 ligand (Promega, G8471). After receptor labeling, media was replaced with fresh serum-free media containing 30nM fluorescently labeled ligands and the cells were incubated for 1 hour. The cell membrane of mESCs without HaloTag-receptors was fluorescently stained with wheat germ agglutinin Alexa Fluor 488 (Thermo Fisher Scientific, W11261) according to the manufacturer's protocol.

Following the 1-hour ligand treatment, cells were fixed with 4% paraformaldehyde (Biotium, 22023). For lysosomal staining, cells were permeabilized with ice-cold methanol at -20°C for 10 minutes, blocked in 10% BSA in PBS for 1 hour at room temperature, and stained with FITC anti-LAMP1 antibody (Abcam, ab24871) at 1:200 dilution overnight at 4°C. After fixation or after LAMP1 staining, ProLong Diamond Antifade Mountant with DAPI (Thermo Fisher Scientific, P36971) was added to stain cell nuclei. The cells were then imaged under a confocal microscope at 100x magnification (Zeiss, LSM710).

Live cell imaging

HEK293 cells expressing human ACVR1-GFP were stained with Lysopainter (Abcam, ab176829) and Hoechst (ThermoScientific, 62249). Live cell imaging was done using Zeiss LSM880 confocal microscope equipped with a humidified and temperature-controlled incubation chamber. The GFP signal was bleached, followed by the addition of 30nM Activin A. Internalization of ACVR1-GFP was then monitored for a duration of 30 minutes. Co-localization of ACVR1-GFP and Lysopainter was calculated using the ZenBlue software.

Cell lines, culture conditions, and transfections

HEK293 and W20 cell lines were cultured in DMEM, supplemented with 10% (v/v) FBS, 50U/mL penicillin/streptomycin, and 2mM L-glutamine in a humidified 37°C incubator with 5% CO_2. Transfection of the HEK293 cells was carried out using the TransIT-293 DNA transfection reagent (MirusBio, MIR 2700), following the manufacturer's recommended protocol.

Immunoprecipitation

The HEK293 cells were transfected with HA-human ACVR2B (HA-ACVR2B) and either myc-human ACVR1 (myc-ACVR1) or myc-human ACVR1.R206H (myc-ACVR1.R206H). After a period of 48 hours, the cells were switched to serum-free DMEM for 1 hour, followed by a treatment with 10nM of ligand for an additional hour. Membrane fractions were then collected using the Mem-PER Plus membrane protein extraction kit (Thermo Fisher Scientific, 89842), in accordance with the manufacturer's instructions. The protein concentration of the membrane fractions and whole cell lysates were measured using the Pierce BCA protein assay kit (Thermo Fisher Scientific, 23227). Myc-tag immunoprecipitation (IP) was carried out using the Myc-tag magnetic IP kit (Thermo Fisher Scientific, 88844), following the manufacturer's recommended protocol.

Ligand treatments and immunoblotting

Forty-eight hours after plating cells, media was switched to serum-free media for 1 hour followed by 1 hour treatment with various ligands or antibodies. Whole-cell lysates were collected with RIPA lysis buffer (Thermo Fisher Scientific, 89901) containing 2X protease and phosphatase inhibitor (Thermo Fisher Scientific, 78440) and 0.1U/mL nuclease (Thermo Fisher Scientific, 88701). Equal amounts of lysates were resolved under reducing conditions in 4%-20% Novex WedgeWell gels (Invitrogen) and transferred to PVDF membranes (Advansta, L-08004-010). Membranes were blocked for 2 hours at room temperature with SuperBlock T20 blocking buffer (Thermo Fisher Scientific, 37536) and incubated with primary antibodies at a 1:1000 dilution (anti-P-Smad1/5 [clone 41D10], anti-P-Smad2 [clone 138D4]), 1:4000 dilution (anti-Myc [clone 71D10], anti-HA [clone C29F4]), or 1:10,000 dilution (anti-cyclophilin B [clone D1V5J]) overnight at 4°C. Membranes were then incubated with horseradish peroxidase-conjugated secondary antibody at a range of dilutions from 1:2000 – 1:10,000 (depending on the primary antibody) for 2 hours at room temperature. Western Bright ECL HRP substrate was used for detection (Advansta, K-12045-D20). Band intensities of the western images were analyzed using ImageJ.

Luciferase reporter assay

Stable pools of HEK293-BRE-luciferase (Smad1/5-responsive) and HEK293-CAGA-luciferase (Smad2/3 responsive) reporter cells were generated. Approximately 8,000 cells were plated in a 96-well plate in complete media. Media was replaced with serum-free DMEM, supplemented with 2mM L-glutamine,

50U/mL penicillin/streptomycin, and 0.1% BSA, twenty-four hours post-plating. Following an overnight starvation period, ligands at various concentrations were added. After 16 hours, luciferase expression was measured using the Bright-Glo luciferase assay system (Promega, E2650).

References

1. Jia, S. & Meng, A. TGFbeta family signaling and development. *Development* **148** (2021).
2. Nickel, J. & Mueller, T.D. Specification of BMP Signaling. *Cells* **8** (2019).
3. David, C.J. & Massague, J. Contextual determinants of TGFbeta action in development, immunity and cancer. *Nat Rev Mol Cell Biol* **19**, 419-435 (2018).
4. Aykul, S. *et al.* Anti-ACVR1 antibodies exacerbate heterotopic ossification in fibrodysplasia ossificans progressiva (FOP) by activating FOP-mutant ACVR1. *J Clin Invest* **132** (2022).
5. Kokabu, S. *et al.* BMP3 suppresses osteoblast differentiation of bone marrow stromal cells via interaction with Acvr2b. *Mol Endocrinol* **26**, 87-94 (2012).
6. Sakuma, R. *et al.* Inhibition of Nodal signalling by Lefty mediated through interaction with common receptors and efficient diffusion. *Genes Cells* **7**, 401-412 (2002).
7. Lewis, K.A. *et al.* Betaglycan binds inhibin and can mediate functional antagonism of activin signalling. *Nature* **404**, 411-414 (2000).
8. Brule, E. *et al.* TGFBR3L is an inhibin B co-receptor that regulates female fertility. *Sci Adv* **7**, eabl4391 (2021).
9. Huning, I. & Gillessen-Kaesbach, G. Fibrodysplasia ossificans progressiva: clinical course, genetic mutations and genotype-phenotype correlation. *Molecular syndromology* **5**, 201-211 (2014).
10. Shore, E.M. *et al.* A recurrent mutation in the BMP type I receptor ACVR1 causes inherited and sporadic fibrodysplasia ossificans progressiva. *Nat Genet* **38**, 525-527 (2006).
11. Hatsell, S.J. *et al.* ACVR1R206H receptor mutation causes fibrodysplasia ossificans progressiva by imparting responsiveness to activin A. *Science translational medicine* **7**, 303ra137 (2015).
12. Hino, K. *et al.* Neofunction of ACVR1 in fibrodysplasia ossificans progressiva. *Proc Natl Acad Sci U S A* **112**, 15438-15443 (2015).
13. Upadhyay, J. *et al.* The Expansion of Heterotopic Bone in Fibrodysplasia Ossificans Progressiva Is Activin A-Dependent. *J Bone Miner Res* **32**, 2489-2499 (2017).
14. Lees-Shepard, J.B. *et al.* Activin-dependent signaling in fibro/adipogenic progenitors causes fibrodysplasia ossificans progressiva. *Nat Commun* **9**, 471 (2018).
15. Di Rocco, M. *et al.* Garetosmab in fibrodysplasia ossificans progressiva: a randomized, double-blind, placebo-controlled phase 2 trial. *Nat Med* (2023).
16. Srinivasan, D. *et al.* How Activin A Became a Therapeutic Target in Fibrodysplasia Ossificans Progressiva. *Biomolecules* **14**, 101 (2024).
17. Attisano, L. *et al.* Identification of human activin and TGFβ type I receptors that form heteromeric kinase complexes with type II receptors. *Cell* **75**, 671-680 (1993).
18. Ebner, R., Chen, R.H., Lawler, S., Zioncheck, T. & Derynck, R. Determination of type I receptor specificity by the type II receptors for TGF-beta or activin. *Science* **262**, 900-902 (1993).
19. Tsuchida, K., Mathews, L.S. & Vale, W.W. Cloning and characterization of a transmembrane serine kinase that acts as an activin type I receptor. *Proc Natl Acad Sci U S A* **90**, 11242-11246 (1993).
20. Piek, E. *et al.* Functional antagonism between activin and osteogenic protein-1 in human embryonal carcinoma cells. *J Cell Physiol* **180**, 141-149 (1999).
21. Aykul, S. & Martinez-Hackert, E. Transforming Growth Factor-beta Family Ligands Can Function as Antagonists by Competing for Type II Receptor Binding. *J Biol Chem* **291**, 10792-10804 (2016).
22. Aykul, S. *et al.* Activin A forms a non-signaling complex with ACVR1 and type II Activin/BMP receptors via its finger 2 tip loop. *Elife* **9** (2020).
23. ten Dijke, P. *et al.* Characterization of type I receptors for transforming growth factor-beta and activin. *Science* **264**, 101-104 (1994).
24. Carcamo, J. *et al.* Type I receptors specify growth-inhibitory and transcriptional responses to transforming growth factor beta and activin. *Mol Cell Biol* **14**, 3810-3821 (1994).

25. Willis, S.A., Zimmerman, C.M., Li, L.I. & Mathews, L.S. Formation and activation by phosphorylation of activin receptor complexes. *Mol Endocrinol* **10**, 367-379 (1996).
26. Macías-Silva, M., Hoodless, P.A., Tang, S.J., Buchwald, M. & Wrana, J.L. Specific Activation of Smad1 Signaling Pathways by the BMP7 Type I Receptor, ALK2. *Journal of Biological Chemistry* **273**, 25628-25636 (1998).
27. Shimizu, A. *et al.* Identification of receptors and Smad proteins involved in activin signalling in a human epidermal keratinocyte cell line. *Genes Cells* **3**, 125-134 (1998).
28. Yamamoto, M., Stoessel, S.J., Yamamoto, S. & Goldhamer, D.J. Overexpression of Wild-Type ACVR1 in Fibrodysplasia Ossificans Progressiva Mice Rescues Perinatal Lethality and Inhibits Heterotopic Ossification. *J Bone Miner Res* **37**, 2077-2093 (2022).
29. Rosen, V. *et al.* Responsiveness of clonal limb bud cell lines to bone morphogenetic protein 2 reveals a sequential relationship between cartilage and bone cell phenotypes. *J Bone Miner Res* **9**, 1759-1768 (1994).
30. Yadin, D., Knaus, P. & Mueller, T.D. Structural insights into BMP receptors: Specificity, activation and inhibition. *Cytokine Growth Factor Rev* **27**, 13-34 (2016).
31. Martinez-Hackert, E., Sundan, A. & Holien, T. Receptor binding competition: A paradigm for regulating TGF-beta family action. *Cytokine Growth Factor Rev* **57**, 39-54 (2021).
32. Agnew, C. *et al.* Structural basis for ALK2/BMPR2 receptor complex signaling through kinase domain oligomerization. *Nat Commun* **12**, 4950 (2021).
33. Mohedas, A.H. *et al.* Structure–Activity Relationship of 3,5-Diaryl-2-aminopyridine ALK2 Inhibitors Reveals Unaltered Binding Affinity for Fibrodysplasia Ossificans Progressiva Causing Mutants. *Journal of Medicinal Chemistry* **57**, 7900-7915 (2014).
34. Zhou, Y. *et al.* Receptor internalization-independent activation of Smad2 in activin signaling. *Mol Endocrinol* **18**, 1818-1826 (2004).
35. Antebi, Y.E. *et al.* Combinatorial Signal Perception in the BMP Pathway. *Cell* **170**, 1184-1196 e1124 (2017).
36. Kitoh, H. Clinical Aspects and Current Therapeutic Approaches for FOP. *Biomedicines* **8** (2020).
37. Nguyen, M.H. *et al.* Discovery of Novel Pyrazolopyrimidines as Potent, Selective, and Orally Bioavailable Inhibitors of ALK2. *ACS Med Chem Lett* **13**, 1159-1164 (2022).
38. Smilde, B.J. *et al.* Protocol paper: a multi-center, double-blinded, randomized, 6-month, placebo-controlled study followed by 12-month open label extension to evaluate the safety and efficacy of Saracatinib in Fibrodysplasia Ossificans Progressiva (STOPFOP). *BMC Musculoskelet Disord* **23**, 519 (2022).
39. Ullrich, T. *et al.* Discovery of a novel 2-aminopyrazine-3-carboxamide as a potent and selective inhibitor of Activin Receptor-Like Kinase-2 (ALK2) for the treatment of fibrodysplasia ossificans progressiva. *Bioorg Med Chem Lett* **64**, 128667 (2022).
40. Lees-Shepard, J.B. *et al.* An anti-ACVR1 antibody exacerbates heterotopic ossification by fibro-adipogenic progenitors in fibrodysplasia ossificans progressiva mice. *J Clin Invest* **132** (2022).
41. Collins, M.T. Twists in the fibrodysplasia ossificans progressiva story challenge and expand our understanding of BMP biology. *J Clin Invest* **132** (2022).
42. Katagiri, T. *et al.* A blocking monoclonal antibody reveals dimerization of intracellular domains of ALK2 associated with genetic disorders. *Nat Commun* **14**, 2960 (2023).
43. Maruyama, R., Nguyen, Q., Roshmi, R.R., Touznik, A. & Yokota, T. Allele-Selective LNA Gapmers for the Treatment of Fibrodysplasia Ossificans Progressiva Knock Down the Pathogenic ACVR1(R206H) Transcript and Inhibit Osteogenic Differentiation. *Nucleic Acid Ther* **32**, 185-193 (2022).
44. Gu, Z. *et al.* The type I serine/threonine kinase receptor ActRIA (ALK2) is required for gastrulation of the mouse embryo. *Development* **126**, 2551-2561 (1999).
45. Mishina, Y., Crombie, R., Bradley, A. & Behringer, R.R. Multiple roles for activin-like kinase-2 signaling during mouse embryogenesis. *Dev Biol* **213**, 314-326 (1999).

46. de Sousa Lopes, S.M. *et al.* BMP signaling mediated by ALK2 in the visceral endoderm is necessary for the generation of primordial germ cells in the mouse embryo. *Genes Dev* **18**, 1838-1849 (2004).
47. Wang, J. *et al.* Atrioventricular cushion transformation is mediated by ALK2 in the developing mouse heart. *Dev Biol* **286**, 299-310 (2005).
48. Rigueur, D. *et al.* The type I BMP receptor ACVR1/ALK2 is required for chondrogenesis during development. *J Bone Miner Res* **30**, 733-741 (2015).
49. Shahid, M. *et al.* BMP type I receptor ALK2 is required for angiotensin II-induced cardiac hypertrophy. *Am J Physiol Heart Circ Physiol* **310**, H984-994 (2016).
50. Matzuk, M.M. *et al.* Functional analysis of activins during mammalian development. *Nature* **374**, 354-356 (1995).
51. Tamm, C., Pijuan Galito, S. & Anneren, C. A comparative study of protocols for mouse embryonic stem cell culturing. *PLoS One* **8**, e81156 (2013).

Extended Data Figures

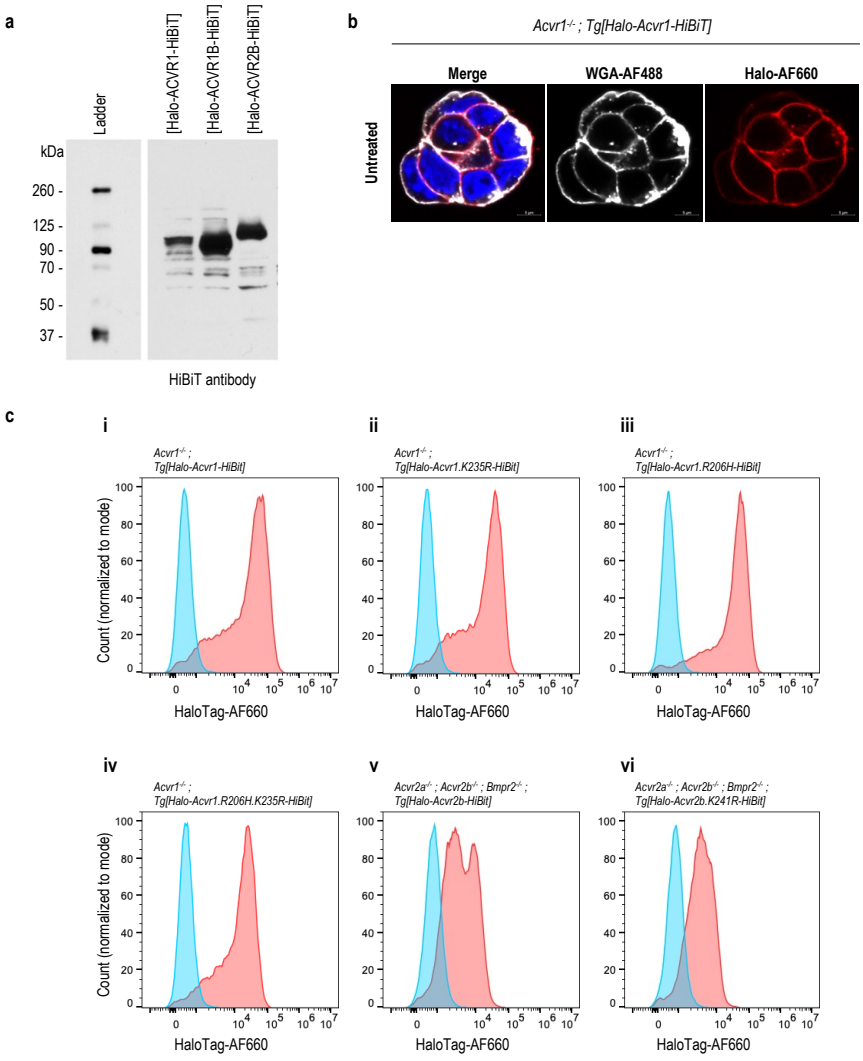

Extended Data Figure 1. Expression of N-terminally Halo and C-terminally HiBiT tagged receptors in mESCs. a, Western blot of Halo-ACVR1B-HiBiT, Halo-ACVR1B-HiBiT, and Halo-ACVR2B-HiBiT. 10µg cell lysate from *Acvr1*$^{-/-}$ mESCs expressing Halo-ACVR1-HiBiT, *Acvr1b*$^{-/-}$ mESCs expressing Halo-ACVR1B-HiBiT and *Acvr2a*$^{-/-}$; *Acvr2b*$^{-/-}$; *Bmpr2*$^{-/-}$ mESCs expressing Halo-ACVR2B-HiBiT were resolved on an SDS-PAGE. The presence of these proteins was detected using a HiBiT antibody. **b**, Halo-ACVR1 localizes on the membrane. *Acvr1*$^{-/-}$ mESCs expressing Halo-ACVR1-HiBiT were stained with AF660 Halo ligand (red) and WGA-AF488 (white) to mark the Halo-ACVR1-HiBit receptor and cell membrane, respectively. Nuclei staining is with DAPI (blue). Confocal microscopy was used for imaging. Co-localization of the Halo tag and WGA staining demonstrates that Halo-ACVR1-HiBiT localizes on the cell membrane. **c**, Cell surface expression of Halo-ACVR1B-HiBiT and Halo-ACVR2B-HiBiT and variants thereof. *Acvr1*$^{-/-}$ mESCs expressing Halo-ACVR1-HiBiT **(i)**, Halo-ACVR1.K235R-HiBiT **(ii)**, Halo-ACVR1.R206H-HiBiT **(iii)**, Halo-ACVR1.R206H.K235R-HiBiT **(iv)**, *Acvr2a*$^{-/-}$; *Acvr2b*$^{-/-}$; *Bmpr2*$^{-/-}$ mESCs expressing Halo-ACVR2B-HiBiT **(v)**, and Halo-ACVR2B.K241R-HiBiT **(vi)** were stained with AF660 Halo ligand and analyzed by flow cytometry. All the tested cell lines showed positive receptor expression on the cell surface. Red curves represent AF660 Halo ligand-stained cells, and blue curves represent unstained cells.

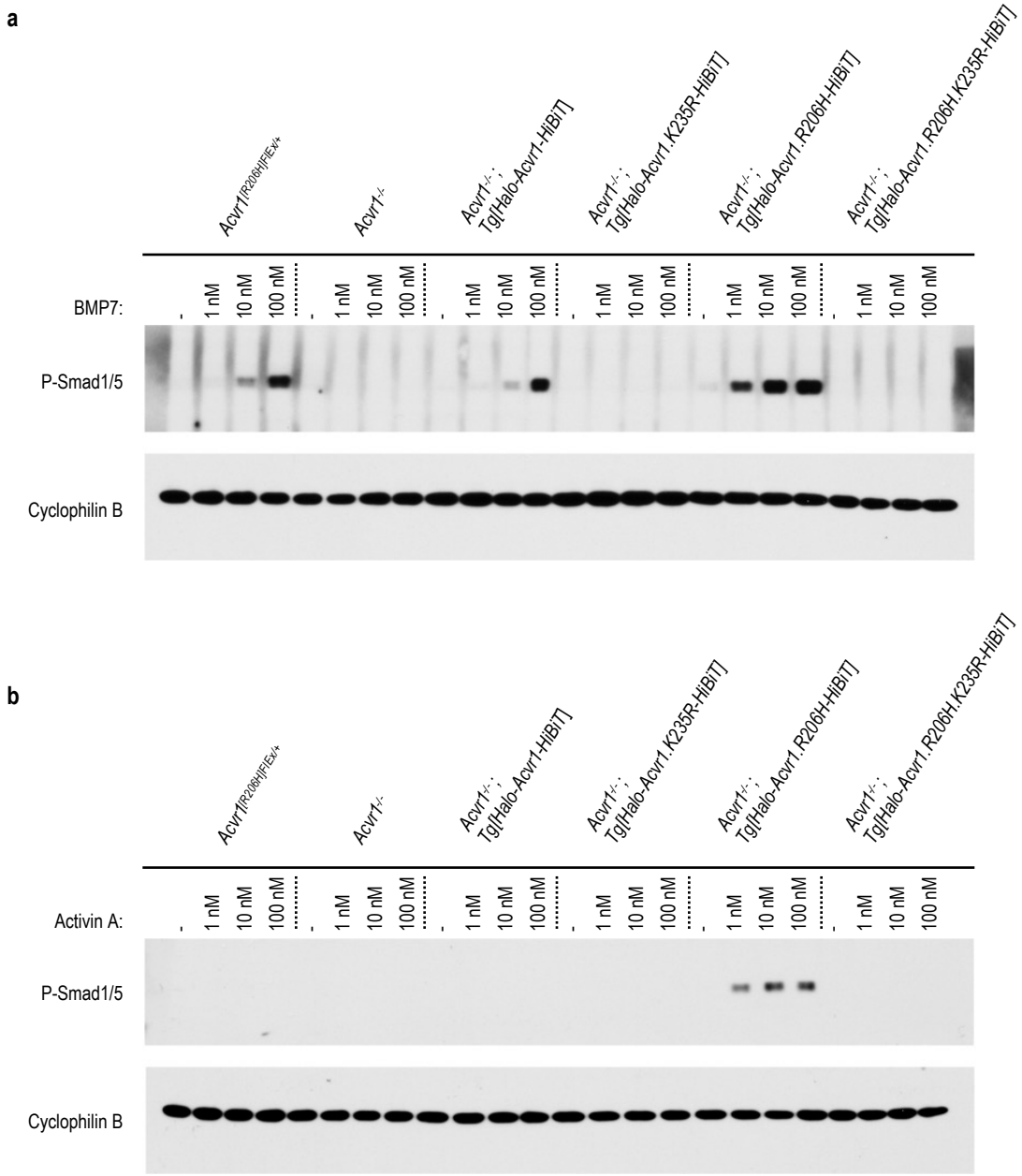

Extended Data Figure 2. Ligand responsiveness of N-terminally Halo and C-terminally HiBiT tagged ACVR1 and variants thereof. a,**b**, *Acvr1*$^{[R206H]FlEx/+}$ mESCs, *Acvr1*$^{-/-}$ mESCs, *Acvr1*$^{-/-}$ mESCs expressing Halo-ACVR1-HiBiT, Halo-ACVR1.K235R-HiBiT, Halo-ACVR1.R206H-HiBiT, and Halo-ACVR1.R206H.K235R-HiBiT were treated with varying concentrations of BMP7 (**a**) or Activin A (**b**) for 1 hour. BMP7 induced Smad1/5 phosphorylation in the parental *Acvr1*$^{[R206H]FlEx/+}$ mESCs, mESCs expressing either wild-type Halo-ACVR1-HiBiT and FOP mutant Halo-ACVR1.R206H-HiBiT, but not in their kinase-dead counterparts, Halo-ACVR1.K235R-HiBiT and ACVR1.R206H.K235R-HiBiT. Activin A induced Smad1/5 phosphorylation only in the FOP mutant Halo-ACVR1.R206H-HiBiT expressing mESCs, but not in its kinase-dead counterpart.

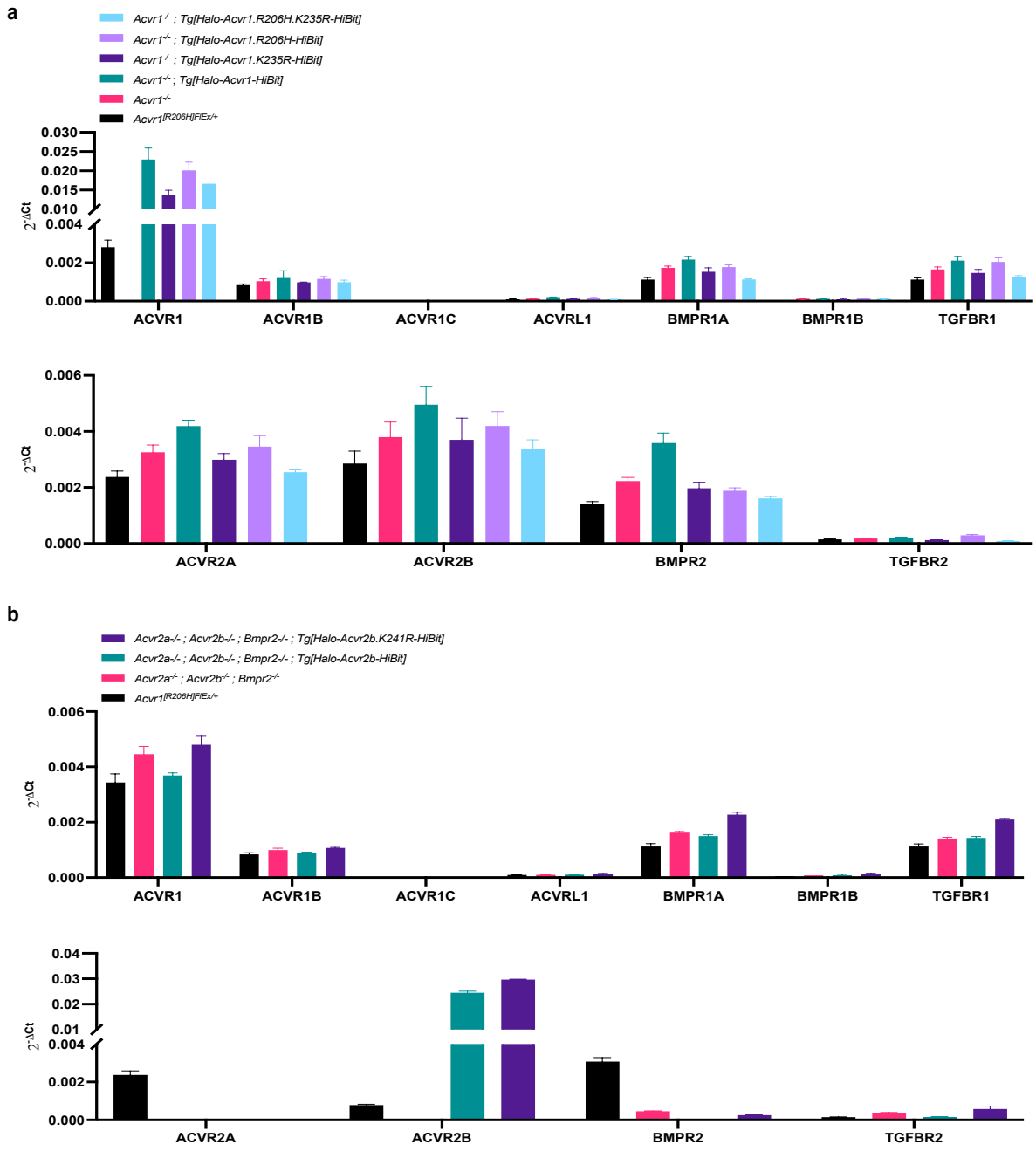

Extended Data Figure 3. Expression levels of type I and type II BMP and TGFß receptors in *Acvr1*$^{-/-}$ mESCs transgenically expressing Halo-ACVR1-HiBiT or Halo-ACVR2B-HiBiT and variants thereof. **a**, Type I and type II receptor mRNA levels of parental *Acvr1*$^{[R206H]FlEx/+}$ mESCs, *Acvr1*$^{-/-}$ mESCs, *Acvr1*$^{-/-}$*; Tg[Halo-ACVR1-HiBiT]* mESCs , *Acvr1*$^{-/-}$*; Tg[Halo-ACVR1.K235R-HiBiT]* mESCs, *Acvr1*$^{-/-}$*; Tg[Halo-ACVR1.R206H-HiBiT]* mESCs, and *Acvr1*$^{-/-}$*; Tg[*Halo-ACVR1.R206H.K235R-HiBiT] mESCs. **b**, Type I and type II receptor mRNA levels of *Acvr2a*$^{-/-}$; *Acvr2b*$^{-/-}$; *Bmpr2*$^{-/-}$ mESCs, *Acvr2a*$^{-/-}$; *Acvr2b*$^{-/-}$; *Bmpr2*$^{-/-}$*; Tg[Halo-ACVR2B-HiBiT]* mESCs, and *Acvr2a*$^{-/-}$; *Acvr2b*$^{-/-}$; *Bmpr2*$^{-/-}$*; Tg[Halo-ACVR2B.K241R-HiBiT]* mESCs. All the N-terminally Halo and C-terminally HiBiT tagged receptors are expressed in the corresponding mESC lines. Expression of the tagged receptors does not affect the mRNA levels of other receptors of the BMP/TGFß family.

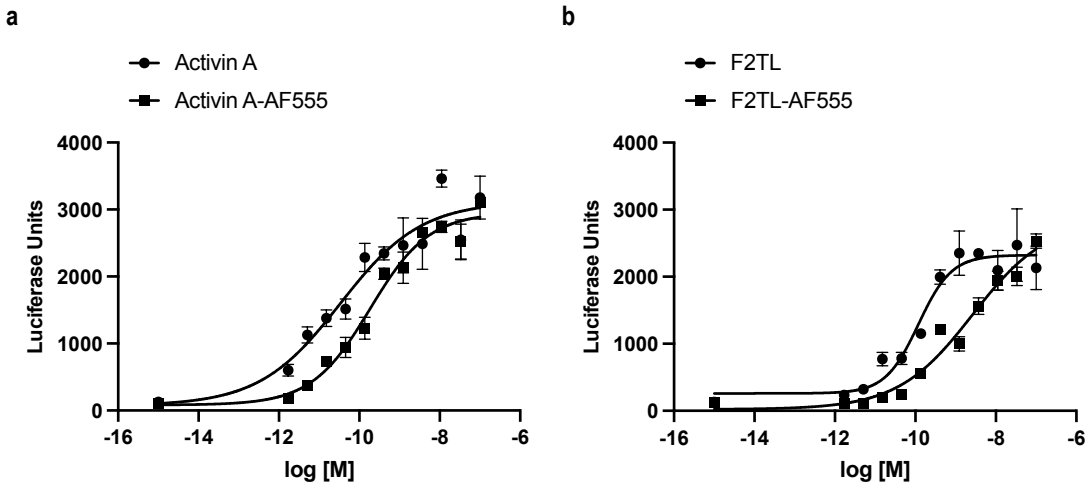

Extended Data Figure 4. Activin A-AF555 and F2TL-AF555 activate Smad2/3 signaling in HEK293-CAGA reporter cells. a,**b**, Activation of Smad2/3 signaling by both unlabeled and Alexa Fluor-555 (AF555) labeled Activin A and F2TL was assessed in HEK293-CAGA luciferase reporter cells (responsive to Smad2/3 signaling). Activin A, Activin A-AF555 (**a**), and F2TL, F2TL-AF555 (**b**) were titrated in the HEK293-CAGA reporter cells. Both unlabeled and AF555 labeled Activin A and F2TL induce Smad2/3 signaling in a similar manner.

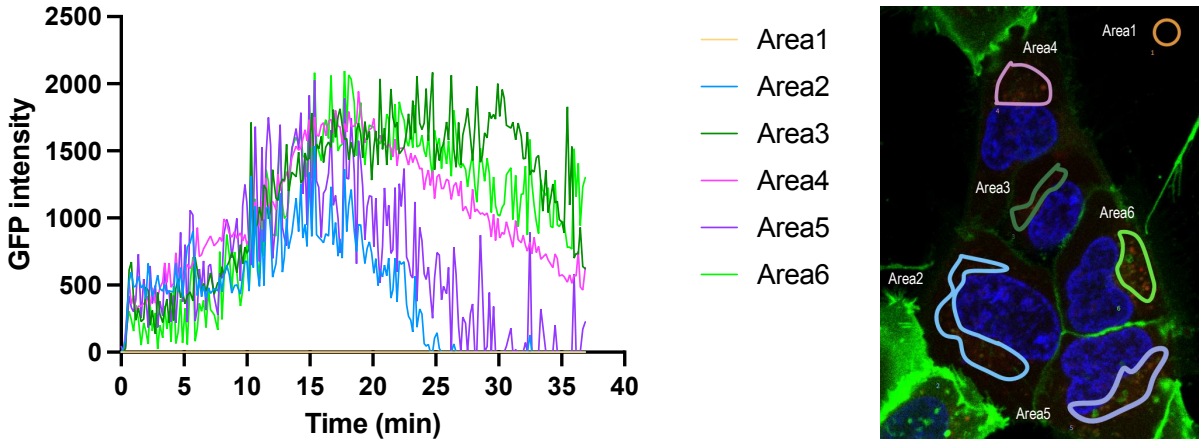

Extended Data Figure 5. Quantification of ACVR1-GFP endocytosis in HEK293[ACVR1-GFP] cells treated with Activin A. Live cell imaging was performed on HEK293 cells overexpressing ACVR1-GFP following lysosome staining with lysopainter. The GFP signal was bleached, and then 30nM Activin A was added. Endocytosis of ACVR1-GFP was quantified over a 30-minute period. Area 1 represents the background fluorescence signal, while areas 2 through 6 represent the amount of internalized GFP signal upon Activin A treatment. The maximum GFP signal was detected 15 minutes after Activin A treatment.

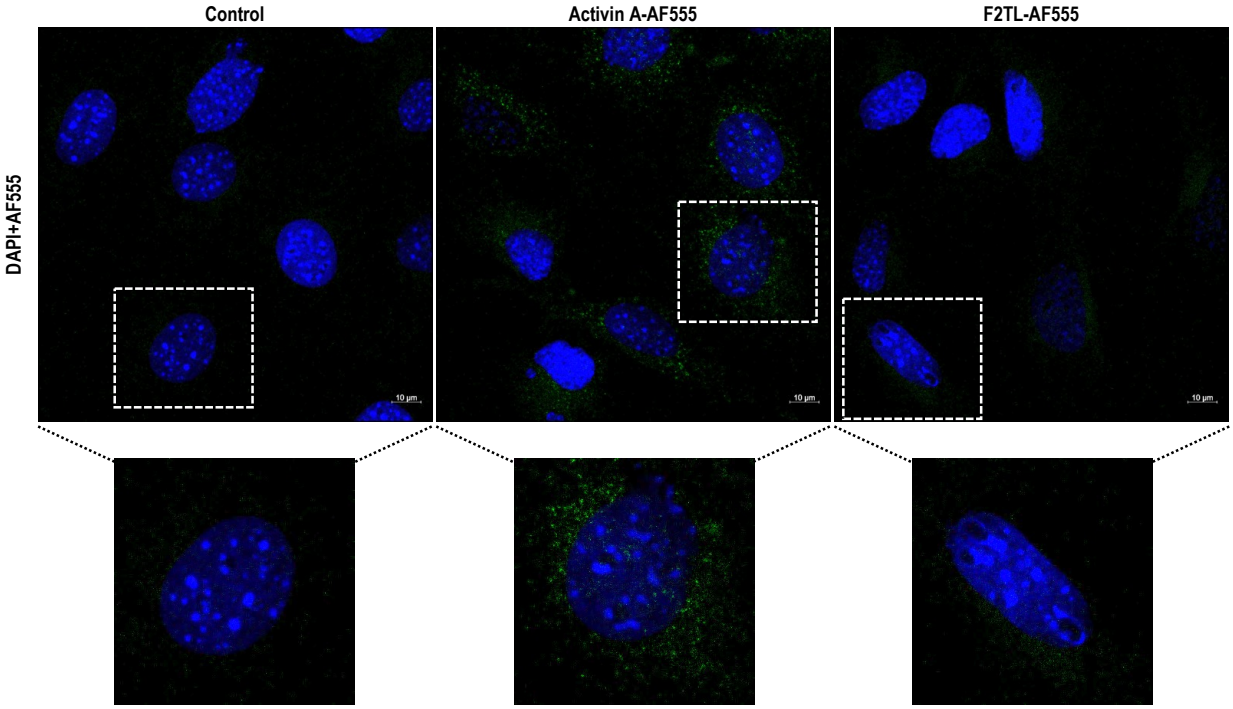

Extended Data Figure 6. Activin A, but not F2TL, undergoes endocytosis in W20 cells. W20 cells were treated with 30nM Activin A-AF555 or F2TL-AF555 or left untreated. The cells were then stained with DAPI (blue) to visualize the cell nuclei. Confocal microscopy was used for imaging, and images from the Z-stack are shown. Activin A-AF555 was endocytosed in W20 cells, but F2TL-AF555 did not.

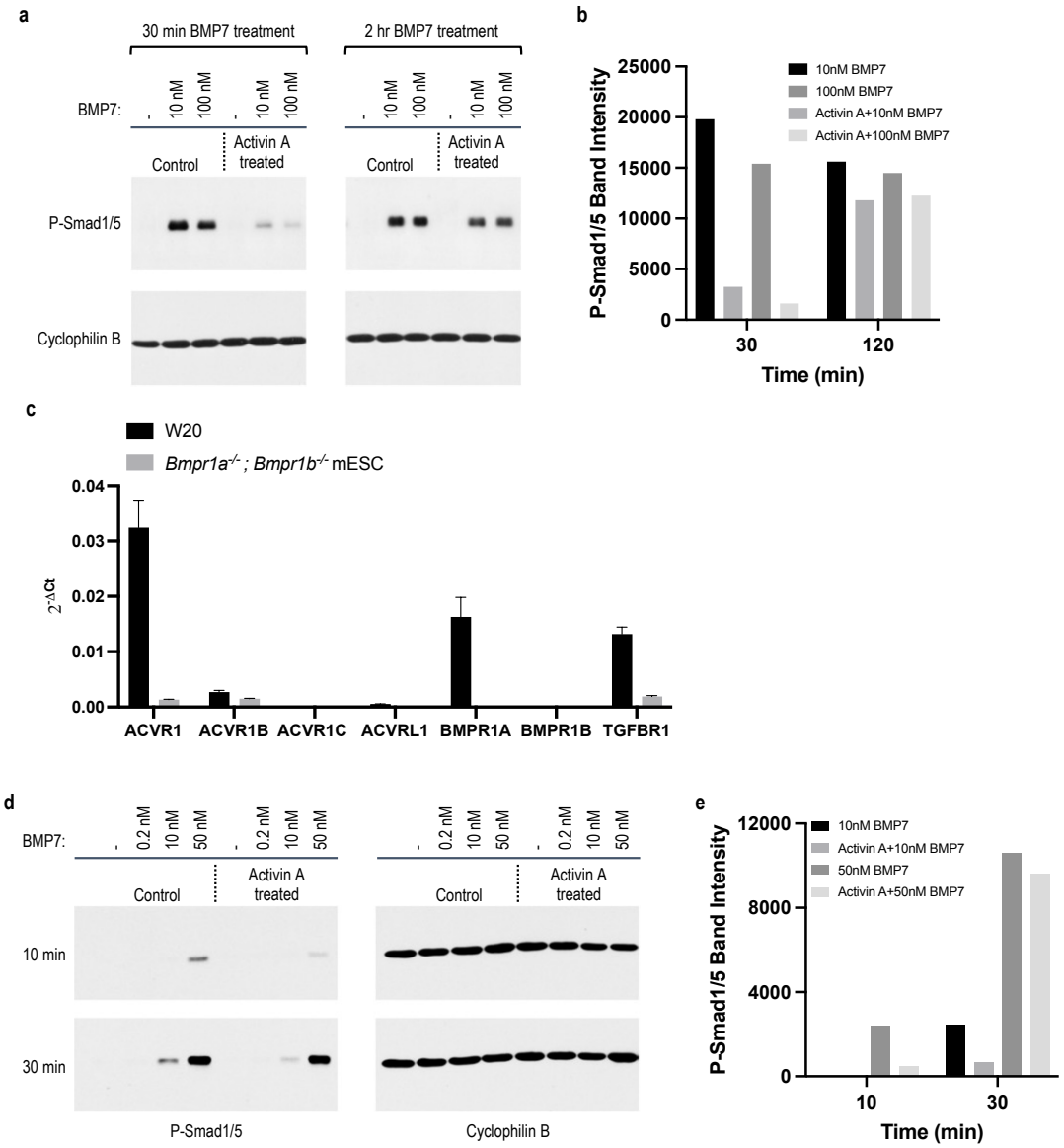

Extended Data Figure 7. ACVR1•Activin A•type II receptor NSCs inhibit BMP signaling in HEK293[myc-ACVR1] and W20 cells. a,**b**, HEK293 cells overexpressing myc-human ACVR1 were either left untreated or treated with 10nM Activin A for 1 hour. After washing off the unbound Activin A, the cells were exposed to varying concentrations of BMP7 for either 30 minutes or 2 hours. Immunoblot analysis (**a**) and quantification (**b**) demonstrate that Activin A significantly decreases BMP7-induced Smad1/5 phosphorylation after 30 minutes. BMP7-induced Smad1/5 phosphorylation recovered 2 hours after the Activin A treatment. **c**, Expression of BMP/TGFß type I and type II receptors in W20 cells and *Bmpr1a*$^{-/-}$; *Bmpr1b*$^{-/-}$ mESCs. Type I receptor mRNA levels of W20 cells and *Bmpr1a*$^{-/}$-; *Bmpr1b*$^{-/-}$ mESCs were analyzed. W20 cells express 10-fold more ACVR1 mRNA and 8-fold more TGFBR1 mRNA than *Bmpr1a*$^{-/-}$; *Bmpr1b*$^{-/-}$ mESCs. The mRNA levels of ACVR1B in W20 cells is similar in both lines. **d**,**e**, W20 cells were either left untreated or treated with 10nM Activin A for 1 hour. After washing off the unbound Activin A, the cells were exposed to varying concentrations of BMP7 for either 10 or 30 minutes. Immunoblot analysis (**d**) and quantification (**e**) show Activin A treatment significantly reduces the BMP7-induced Smad1/5 phosphorylation.

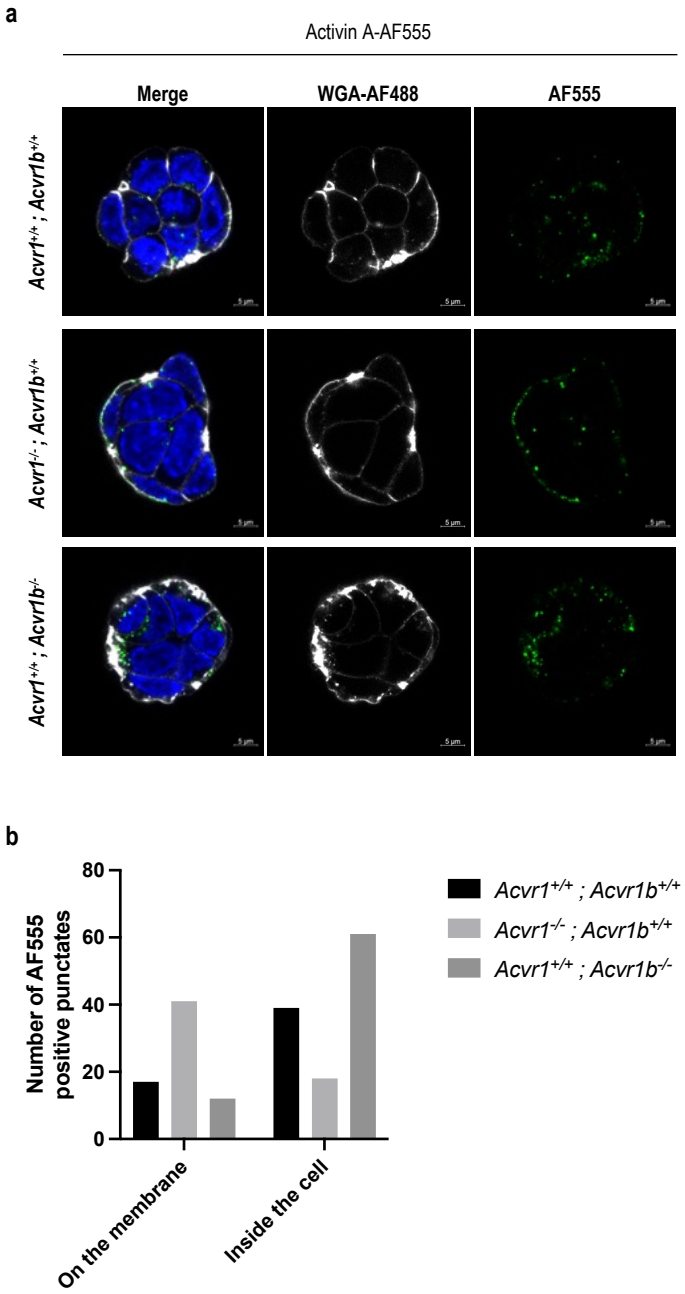

Extended Data Figure 8. ACVR1B is not required for endocytosis of Activin A. Wild type (*Acvr1*$^{+/+}$; *Acvr1b*$^{+/+}$), *Acvr1* knock-out (*Acvr1*$^{-/-}$; *Acvr1b*$^{+/+}$), and *Acvr1b* knock-out (*Acvr1*$^{+/+}$; *Acvr1b*$^{-/-}$) mESCs were either treated with 30nM AF555-labeled Activin A. **a**, Cells were stained with WGA-AF488 to mark the membrane, depicted in white, while AF555 and nuclei staining are represented in green and blue, respectively. Confocal microscopy was used for imaging. Activin A-AF555 did not internalize in *Acvr1* KO mESCs but internalized in *Acvr1b* knock-out mESCs. **b**, Quantification of internalized and membrane-localized Activin A-AF555 was done using Image J.

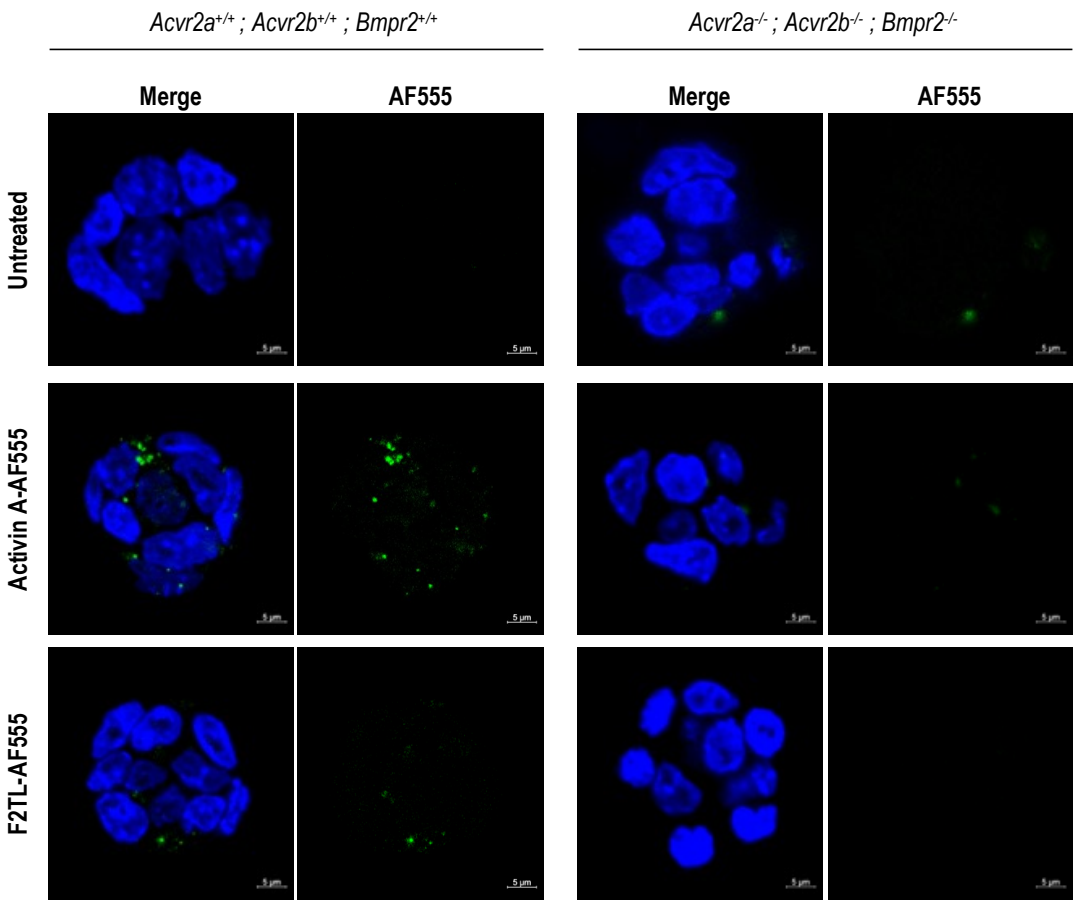

Extended Data Figure 9. Type II receptors are required for endocytosis of ACVR1•Activin A complexes. *Acvr2a*$^{+/+}$*; Acvr2b*$^{+/+}$*; Bmpr2*$^{+/+}$ mESCs and *Acvr2a*$^{-/-}$*; Acvr2b*$^{-/-}$*; Bmpr2*$^{-/-}$ mESCs were treated with 30nM AF555-labeled Activin A or Activin A.F2TL or left untreated. Activin A-AF555 did not internalize in type II receptor knock-out *Acvr2a*$^{-/-}$*; Acvr2b*$^{-/-}$*; Bmpr2*$^{-/-}$ mESCs, but slightly internalized in mESCs expressing endogenous levels of type II receptors. F2TL-AF555 did not internalize in either condition.

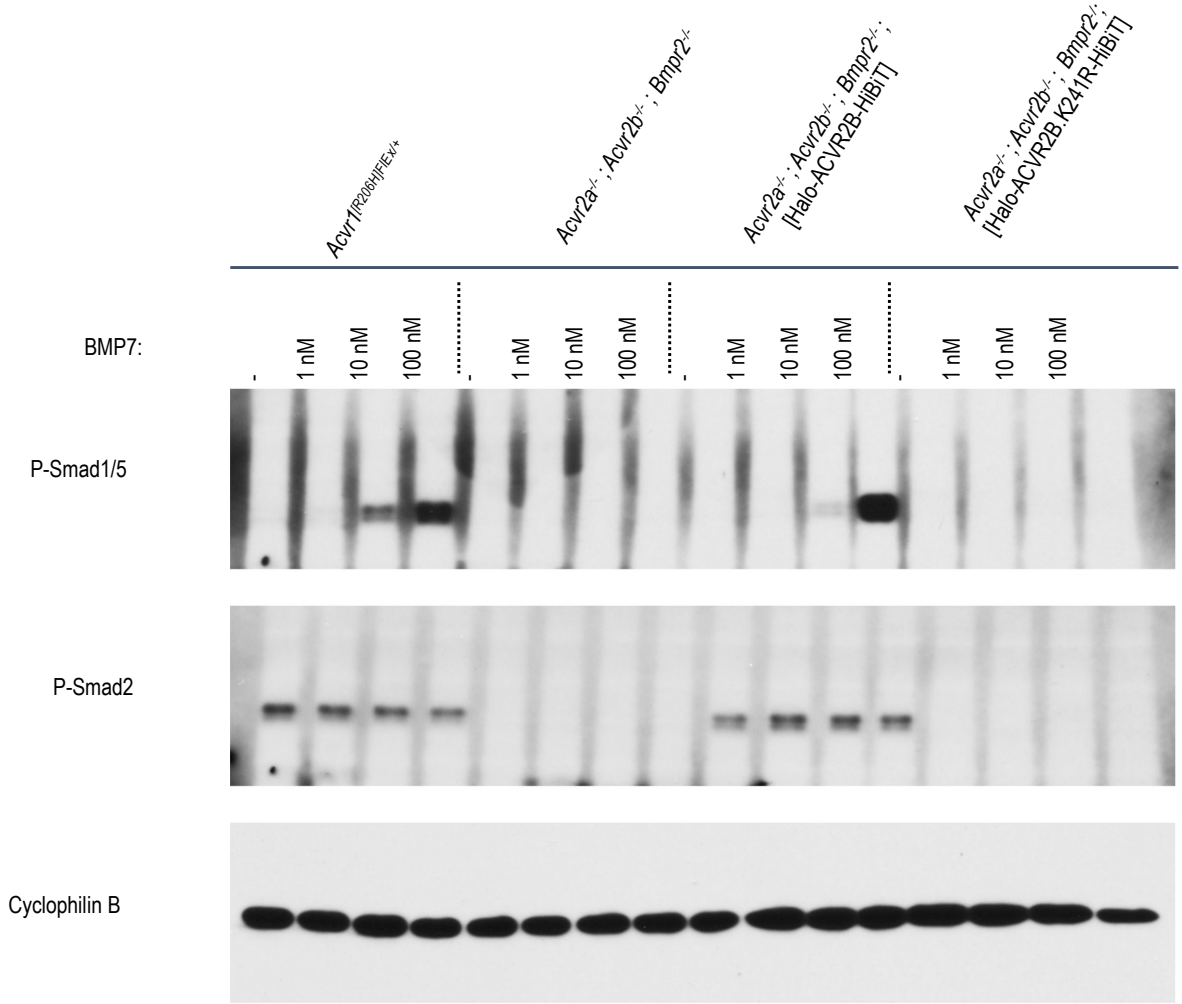

Extended Data Figure 10. BMP7 induces Smad1/5 phosphorylation in Halo-ACVR2B-HiBiT-expressing mESCs. *Acvr1*$^{[R206H]FlEx/+}$ mESCs, *Acvr2a*$^{-/-}$*; Acvr2b*$^{-/-}$*; Bmpr2*$^{-/--}$mESCs, and *Acvr2a*$^{-/-}$*; Acvr2b*$^{-/-}$*; Bmpr2*$^{-/-}$ mESCs expressing Halo-ACVR2B-HiBiT and Halo-ACVR2B.K241R-HiBiT were treated with varying concentrations of BMP7 for 1 hour. BMP7 induced Smad1/5 phosphorylation both in the parental *Acvr1*$^{[R206H]FlEx/+}$ and Halo-ACVR2B-HiBiT expressing mESCs. It did not induce Smad1/5 phosphorylation in the kinase-dead Halo-ACVR2B.K241R-HiBiT expressing mESCs.